A Survey of Channel Modeling for UAV Communications

Aziz Altaf Khuwaja, Yunfei Chen, *Senior Member, IEEE,* Nan Zhao, *Senior Member, IEEE,* Mohamed-Slim Alouini, *Fellow, IEEE* and Paul Dobbins

***Abstract*—Unmanned aerial vehicles (UAVs) have attracted great interest in rapid deployment for both civil and military applications. UAV communication has its own distinctive channel characteristics compared to the widely used cellular or satellite systems. Accurate channel characterization is crucial for the performance optimization and design of efficient UAV communication. However, several challenges exist in UAV channel modeling. For example, the propagation characteristics of UAV channels are under explored for spatial and temporal variations in non–stationary channels. Additionally, airframe shadowing has not yet been investigated for small size rotary UAVs. This paper provides an extensive survey of the measurement methods proposed for UAV channel modeling that use low altitude platforms and discusses various channel characterization efforts. We also review from a contemporary perspective of UAV channel modeling approaches, and outline future research challenges in this domain.**

***Index Terms*—Channel characterization, channel models, measurement campaigns, UAV communication.**

I. Introduction

UNMANNED aerial vehicle (UAV) communication has seen dramatic development in a variety of applications. Most of these applications deploy UAVs as low altitude platforms. In order to ensure safety and high reliability, it is of utmost importance to thoroughly characterize communication channels. Many research organizations and standardization bodies have worked together to establish pragmatic UAV frameworks. For example, in 2013, the special committee (SC–228) has been formed by the Radio Technical Commission for Aeronautics (RTCA) to frame minimum performance standards for UAV operations [1]. RTCA has also established the drone advisory committee in 2016 to ensure the safe introduction of UAVs into the US national airspace system [2]. Also, the National Aeronautics and Space Administration (NASA) and Federal Aviation Administration (FAA) have launched a joint research initiative to integrate UAVs into a national aerospace system across the United States [3].

The most unique features that distinguish UAV communication and characteristics from conventional communication include: a) the highly dynamic communication channels characteristics for air–to–ground (AG) and air–to–air (AA) propagations due to UAV velocity; b) the excessive spatial and temporal variations induced in the non–stationary channels due to the mobility of both the aerial base station and the ground operators; c) airframe shadowing caused by the structural design and rotation of the UAV.

In the diverse propagation environment where UAVs operate, these features become more challenging. The main difference between UAV communications with aerial base stations deployed in 3D space and conventional cellular communications with fixed base stations installed in 2D plane is that the aerial base station movement can proliferate problems with coverage and connectivity by inducing severe non–stationarity. UAV can also be a viable solution to a wireless recovery network in cases of terrestrial disruption. Also, compared with satellite communication, UAV is cost–effective, having lower latency and better signal–to–noise ratio. Propagation characteristics for terrestrial cellular systems are often corroborated using well–established empirical and analytical models. The satellite links for land mobile systems have also been thoroughly investigated in the literature [4],[5]. However, for different system structures and operations, these models are often not well suited for characterizing UAV channels. To this end, UAV communication is still in its infancy and no well–established standard has been proposed.

Reliable analytical models are necessary to evaluate the performances of different wireless techniques. Generally, for AG channels in UAV communication, modeling approaches can be classified into three categories. The first approach is to develop deterministic models using environmental parameters. Such models are useful for studying large–scale fading effects in the channel [6],[7]. Hence the propagation conditions [8],[9] can provide coverage analysis and indicate the optimal UAV position [10]-[12]. The second approach is to develop a tapped delay line (TDL) model to characterize the direct path as well as the multipath components. Then wideband frequency–selective parameters can be derived from the channel impulse response [13]–[15]. This approach is particularly important if non–stationarity exists in the AG channel. Finally, geometric–based stochastic models are desirable for evaluating spatial–temporal characteristics in a geometric simulation environment. This approach is preferable for characterizing the

Manuscript received November 25, 2017; revised

Aziz Altaf Khuwaja is with the School of Engineering, University of Warwick, Coventry, U.K. CV4 7AL and also with the Department of Electrical Engineering, Sukkur IBA University, Sukkur, Sindh, Pakistan (e-mail: A.khuwaja@warwick.ac.uk).

Yunfei Chen is with the School of Engineering, University of Warwick, Coventry, U.K. CV4 7AL (e-mail: Yunfei.Chen@warwick.ac.uk).

Nan Zhao is with the School of Information and Communication Engineering, Dalian University of Technology, China (e-mail: zhaonan@dlut.edu.cn). *(Corresponding author: Nan Zhao.)*

Mohamed-Slim Alouini is with the King Abdullah University of Science and Technology (KAUST), Thuwal 23955-6900, Makkah Province, Kingdom of Saudi Arabia (e-mail: slim.alouini@kaust.edu.sa).

Paul Dobbins is with Telent Co. U.K., Haywood Road, Warwick, CV34 5AH, U.K. (e-mail: paul.dobbins@telent.com).

AG channel in a 3D plane with less environmental parameters [16]-[21].

However, empirical studies are essential to authenticate or disprove theoretical models. Practically the choice of aerial platform in terms of its altitude has presented some opportunities and challenges. High altitude UAVs are capable of operating in the upper layer of the stratosphere [22] where the coverage performance is completely dependent on line–of–sight (LOS) propagation, and marginally relies on the elevation angle. Atmospheric effects and propagation delay are bottlenecks in their modeling, but high altitude platforms can expand the UAVs coverage and provide a generic communication framework of aerial heterogeneous networks. In contrast, for low altitude platforms, the deployment of commercial UAVs are limited by civil aviation regulations [23]. For instance, a maximum limit of 120 m is permitted by the FAA in USA [24] and the Civil Aviation Safety Authority (CASA) in Australia [25]. This altitude range is feasible for power–limited UAVs to meet the quality–of–service requirements of end–users confined within the small cells. In this case, optimum placement of the UAV and the characteristics of the environment determine the major channel parameters. However, the power consumption and endurance time of UAVs are the performance limitation factors for both cases. Most of the work reported in the literature [26]-[40], are pertinent to AG channel characterization based on measurements with manned aircrafts at high altitude platform. However, these findings cannot be directly applied to single–hop UAV networks deployed at low altitude due to the demand for a high data rate, low latency and continuous connectivity. It is evident from the studies in [41]–[68] that the impact of the UAV placement and the surrounding environments is significant for the propagation characteristics of UAV communications due to time and frequency selectivity in the dynamic UAV channels and can lead to fading. However, less research efforts have been made to tackle shadowing induced in AG and AA channels by the UAV's structural design and maneuvering. In addition, the wide–sense stationary uncorrelated scattering (WSSUS) assumption may be violated in some UAV–aided applications. Thus, in order to avoid over exaggerated performance evaluation from analytical and empirical channel models, it is important to estimate the fading statistics within stationary intervals. Unlike the AG channel, the AA propagation channel is predominantly important in multi–hop UAV networks for sensing and coordination applications, and for back–haul wireless connectivity to complement existing communication systems. Moreover, the propagation characteristics of AA channels are similar to that in free space and largely dependent on strong LOS conditions and ground reflection effects. In the literature, the AA propagation channel has been empirically characterized using low power radios based on the IEEE 802.15.4 [54]–[56] and IEEE 802.11 standards [57],[59]. But these studies only reported large–scale fading statistics, while the impact of antenna orientation and the Doppler spectrum of the AA channel are largely unstudied.

Despite the importance of channel modeling in UAV communications, very few survey studies are available in the literature. For instance, reference [69] identified key issues related to the formation of multi–UAV network, but this survey focuses more on the communications and especially the control of the UAV. Aerial networking characteristics and requirements were reviewed in [70] for civil applications, however, this survey mainly discussed the communications aspects of UAVs, in particularly network layer designs. Both [69] and [70] barely touch on channel modeling. On the other hand, the physical layer characterization of the AG channel at the L and C bands was comprehensively reviewed in [71]. However, practical measurements reported in this paper were mainly for aeronautical communications and land mobile satellite systems in the L and C bands. In contrast, our survey review current advances in UAV channel characterization.

The rest of the paper is organized as follows. In Section II, we review the measurement techniques proposed for UAVs as low altitude platforms. The characterization of AA and AG propagation using empirical channel models are discussed in Section III. In Section IV, we categorize the analytical UAV channel models as deterministic, stochastic, and geometry–based. In Section V, we highlight some important issues pertinent to airframe shadowing, non–stationary channels, and applicability of diversity techniques in UAV communications. In Section VI, we discuss future research challenges for UAV measurements and channel modeling.

II. Measurement Campaigns

The actual behavior of the propagation channel can be better understood via field measurements. UAV channel characterization mainly depends on the operational environment, propagation scenario (AG or AA), channel sounding process, antenna orientation, placement and flight dynamics.

In the literature, most of the measurement campaigns have been conducted using two types of aerial vehicles. The first type are small and medium sized manned aircraft. For instance, in [13]-[15], a S–3B Viking aircraft was used to comprehend the AG channel characteristics at the L and C bands in different environments. In [31], a Cessna–172S aircraft was used to evaluate the performance of a 4×4 multi–input multi–output (MIMO) enabled orthogonal frequency–division multiplexing (OFDM) system for the AG channel. In [32] and [33], a UH–1H military helicopter was used to study the AG channel in a 4×2 MIMO configuration to achieve the diversity gain and to mitigate inter–symbol interference in frequency–selective channels. In [34], a news–reporting helicopter was used to attain spatial multiplexing gain and throughput for airborne communication in 2×2 MIMO settings. The logistics involved in the measurement campaigns using manned aircraft are expensive and daunting. Therefore, the second type of aerial vehicles i.e., UAVs are preferable to reduce the cost. In this case, the UAV payload is often integrated with an on–board processor to control flight dynamics and wireless equipment to collect data. In addition, the experimental setup also contains antennas to radiate and receive radio frequency (RF) signals, global positioning system (GPS) system to record telemetry data, and a inertial measurement unit (IMU) to measure flight dynamics such as pitch, yaw and roll angles. In the rest of the paper, we mainly focus on measurement campaigns using UAVs.

A. Narrowband and Wideband Channel Sounder

1) Narrowband Measurement Systems: These systems evaluate the Doppler frequency shift and the channel gain experienced by narrowband continuous wave (CW) signals using a channel sounder that generates pilot tones at a single carrier frequency. Examples of narrowband measurement campaigns for characterizing the AG propagation channels in aeronautical communications for the very high frequency (VHF) band are given in [35],[36], for L band in [37] and for higher frequency (HF) band in [38].

In [41], the measurement campaign was performed in an urban area of Prague, Czech Republic, using a 2 GHz CW transmitter with a bandwidth of 12.5 kHz. The airship UAV flew between 100 to 170 m above the ground level at a low elevation angle between 1° to 6°. The authors have statistically characterized the AG channel which fits between a purely terrestrial link and a land mobile satellite system. They have also presented a narrowband channel estimator capable of replicating the signal dynamics. Some related measurement campaigns were conducted with similar equipment in Prague for a path loss model in an urban area [42] with a flight altitude between 150 to 300 m. Further, measurements in [43] and [44] were obtained in urban and wooded areas, respectively, to study space diversity techniques.

In [45], field experiments were performed in suburban Madrid, Spain, at frequency band of 5.76 GHz for narrowband measurements. The UAV flew at an altitude between 0 to 50 m for the vertical flight test in ascending and descending directions and covered a distance of 210 m for a horizontal test at altitudes of 20 m and 30 m in two different zones. The authors have investigated large–scale fading effects in the UAV propagation channel and computed path loss exponent for both vertical and horizontal directions using the dual slope and the log–distance path loss models, respectively. They found that, during the vertical flight, the attenuation decreased below the breakpoint distance and then increased with UAV altitude. Whereas, the attenuation increased exponentially with the horizontal flight direction.

These works have studied AG propagation for variations in channel gain with respect to the elevation angle using the Loo model in [41] and the impact of UAV during the course of vertical and horizontal flight routes on fast fading of Rician distribution in [45]. However, channel features were not addressed with regard to the geographical environment, such as density and shape of surrounding scatters. Also, the Doppler behavior of the AG channel was not investigated, which is the key parameter that may differentiate UAV channels from the conventional wireless channel. Therefore, more measurements are required for characterizing the AG propagation with the environmental effects and the maneuvering of UAVs. Moreover, these campaigns conducted with narrowband measurement systems which are only appropriate for computing frequency non–selective fading parameters, as they lack the temporal resolution needed to distinguish closely arriving paths and hence, may not be suitable in a rich multipath environment.

2) Wideband Measurement Systems: These systems determine the channel impulse response (or transfer function) and frequency–selective parameters, such as delay spread. In addition, the power delay profile is acquired from the collection of channel impulse responses to determine the fading statistics for an in–depth insight into the average power carried by the multipath components with a certain delay and the available frequency diversity. As a result, different transmission schemes can be tested to combat small–scale fading in UAV channels. Wideband channel measurements for characterizing the aeronautical propagation channels are mostly conducted with a spread spectrum channel sounder. One such type is the correlative channel sounder, where a pseudonoise (PN) sequence is transmitted as the channel sounding signal, and the received signal is then correlated at the receiver with the same PN sequence. As a result, fading statistics for the time–invariant channel can be captured from the output of the receiver correlator by performing a convolution between the PN sequence and the channel impulse response. This process is usually performed off–line using computational resources. From the perspective of aeronautical communication, a correlative channel sounder was used in [39] and [40] for measuring multipath effects. In the context of characterizing the UAV propagation channel, the wideband frequency–selective parameters are often measured using the universal software radio peripheral (USRP) hardware platform, for instance, as in [45],[46] and [48]. This platform provides more flexibility in terms of low–power consumption and multiple frequency bands.

In [45], the wideband measurement campaign was performed with the channel sounding signal generated by a LTE base station at a frequency of 1.817 GHz. In this work, the small–scale variations in the UAV propagation channel was characterized with the measured channel impulse response, the estimated delay spread and power delay profile. The authors have analyzed the fading statistics, and consequently qualitative performance of the AG propagation using the empirical cumulative distribution function (CDF). They found a random behavior of the multipath components at different UAV altitudes. However, comparison analysis of empirical CDF with the fading channel distributions was not performed. Therefore, this work was extended in [46] to a propose channel modeling approach based on a machine learning and estimated channel parameters with regard to the environment. The Rician K factor was evaluated as a piece–wise function of altitude. However, the Doppler spread was not estimated due to low airspeed of the UAV.

In [47], the measurement campaign was conducted for open and suburban spaces on the campus of Florida International University using an ultra–wideband (UWB) channel sounding radio. In the first scenario, the receiver was placed under the tree canopy at 1.5 m above the ground. In the second scenario, the receiver was placed at the same height with clear LOS to the transmitter. In the third scenario, the receiver was lowered to 7 cm from the ground in a LOS condition. For all these three receiver settings, the UAV transmitter was raised from 4 m to 16 m above ground with a step size of 4 m. In this work, the authors have characterized the AG propagation channel. They proposed the empirical path loss model for both static and mobile UAVs. They found the worst path loss attenuation for the mobile UAV in the first scenario, whereas, the best for the static UAV in the second scenario. They characterized the fading channel as Nakagami–m distributed and a presented multipath propagation model.

In [48], the measurement campaign was performed in both a residential area and a mountainous desert landscape in Arizona, USA. The software defined radio (SDR) platform was tuned to 5.8 GHz. The authors have characterized the frequency–selectivity of the AG propagation by the average and RMS delay spread of the channel. Also, the time–selectivity in terms of the Doppler power spectrum was calculated by summing the entire range of the scattering function delay. They analyzed the channel statistics with the CDF and found that the desert terrain caused substantial delay spread in the AG propagation compared to the residential area. Moreover, CDF analysis followed a log–normal trend for the RMS Doppler spread. However, this work studied the variations in the channel due to time and frequency selectivity effects, and did not provide an empirical model for fading channel distributions.

These studies have characterized the AG channel for small–scale variations in hovering and mobility of the UAV in space, but did not take into account ground reflected multipath components during the landing and take–off phases. In addition, these works ignored the non–stationarity of the AG channel while estimating the fading statistics. Therefore, future wideband measurements should address these challenges for the accurate characterization of the UAV propagation channel. Due to their better multipath resolution, wideband measurements are more desirable for acquiring both time and frequency–selective fading parameters. However, additional computational capabilities are required to process the raw data collected from the measurements. Therefore, this type of measurement system may not be suitable for real–time characterization of the fading channel parameters. Also, the cost and physical dimensions of wideband channel sounding equipment are constraints that need to be considered.

B. IEEE 802.11 based UAV Measurements

UAV channel characterization using commercial off–the–shelf 802.11 radios are desirable due to their low power consumption, cost effectiveness and flexibility to be integrated with small size UAVs. Furthermore, these radios are mostly utilized to form single–hop and multi–hop UAV networks. For these reasons, single–hop UAV networks are usually desirable for characterizing the propagation channel between a single UAV and the ground station or between two UAVs. On the other hand, multi–hop UAV networks are preferable for studying inter–UAV communication either in mesh or star topologies controlled by the ground station. However, the performances of such radios are prone to interference and background noise. Fixed narrowband frequency and limited communication range are other constraints affecting the evaluation of fading channel parameters. Channel characterization efforts reported in the literature for multi–hop UAV networks were based on IEEE 802.11 in [49]-[53] and also IEEE 802.15.4 ZigBee devices in [54]-[56]. In this section we mainly review the measurement campaigns relevant to 802.11 radios for single–hop UAV networks. Section III will highlight the empirical relevance of multi–hop UAV networks from the perspective of both the AA and AG channel modeling.

In [57], the measurement campaign was performed in the laboratory and outdoor environments to study, in particular, the altitude–dependent multipath propagation in the AA channel. The measurements were collected with 802.11 a/b/g/n WLAN devices from two different vendors and deployed in three outdoor scenarios using a hexacopter UAV. In the first scenario, the impact of flight distance followed a free space path loss model. In the second scenario, yaw angle was considered with a good signal reception attained between 170°–230° and the worst signal for an angle of 240°–260°. Finally, the effect of the ground reflected multipath components on UAV altitude was examined for a flight altitude between 10 to 40 m and the height–dependent Rician model was proposed with a K factor reliant on the UAV altitude.

In [58], the measurement campaign was performed for both an open area and a campus environment using a quadcopter UAV and an access point (AP) connected with a 802.11a WLAN interface at a frequency of 5.240 GHz, where the UAV flight altitude varied between 20 and 120 m. Two vertically polarized omni–directional antennas were mounted on both UAV and AP. This study analyzed the impact of flight dynamics and antenna orientation on the AG propagation channel and found that the optimal antenna orientation can alleviate the impact of UAV hovering and mobility on received signal strength and throughput. On one hand, horizontally aligned antennas reduced the effect of UAV yaw difference due to improved antenna alignment gain. On the other hand, vertically aligned antenna handled the impact of UAV acceleration and deceleration against the tilting. Furthermore, they also found that the propagation condition followed that of free space for an open field. This work was extended in [59] using the 802.11a (5.240 GHz) standard to study the network performance and fading channel statistics for AA and AG propagations. Measurements were collected with three horizontally aligned dipole antennas at a flight altitudes between 15 and 110 m. The authors observed that for both AG and AA channels, the path loss exponent computed by the log–distance model matched roughly with that of free space propagation. The Nakagami–m distribution was found to be a good fit for a multipath fading channel in AG propagation. Furthermore, the quality of UAV channels in terms of throughput variations over distance intervals was analyzed using the inter–arrival time of packet and retransmission attempts. As a result, inter–arrival time was under 1 ms for all distances. The number of retransmissions required for distances between 300 to 400 m were not more than 85% for most of the time.

In [60], the measurement campaign was conducted at a private airfield in Connecticut, USA, using a 802.11a radio mounted on a fixed–wing UAV. The UAV flew at approximately 64 km/h and maintained an altitude of roughly 46 m over the ground receiver nodes. The authors evaluated the throughput and reported the highest rates were with a horizontal dipole, orthogonal to flight direction and parallel to the ground. In addition, they also estimated that the path loss roughly followed that of free space propagation. A related measurement campaign was performed in [61] using 2.4 GHz 802.11g and 5.8 GHz 802.11a devices. In this case, the authors computed the maximum range attained with a 802.11a radio and compared this with 802.11g. They found that a 802.11g node can provide robust communication at an altitude of approximately 183 m. In this work, another experimental trial was conducted with a 900 MHz 802.11 radio to determine the communication range performances in comparison to 802.11a/b/g. They found a significant communication range of up to 2000 m with throughput in Mbps by analyzing the slope of a linear regression applied to the received signal strength. In [67], the measurement campaign was performed in a farmland area surrounded by woods. In this work, AG channel characterization was determined in terms of network level diversity gain, and they found a significant enhancement in packet transmission rate by using multiple receivers.

These studies have mostly focused on measuring the attenuation of the received signal strength and throughput of the AG propagation using omni–directional antennas. It is evident from these campaigns that IEEE 802.11 low–power radios can provide opportunities for characterizing UAV propagation channels that have novel designs. Different types, orientations and placements of antenna on UAVs can be studied. Moreover, these radios are preferable for estimating the bit error rate performance and latency in UAV networking. However, analysis of spatial and temporal variations was not comprehensively studied in these works due to a lack of frequency resolution. Also, in a complex communications environment where UAV operates, interference from other 802.11 equipment can be challenging. In this case, one possible solution is to optimize altitude and inter–UAV distance to attain high signal–to–interference–plus–noise ratio (SINR) in the physical layer for a short period of time. Otherwise, interference management techniques may be needed.

C. Cellular–Connected UAV Measurements

Cellular networks can be considered as a prospective candidate to facilitate UAV applications in civil and commercial domains. The widely deployed cellular infrastructure can be utilized to provide reliable AG channels, and hence cut the cost of investing additional ground infrastructure and spectrum allocation. However, since cellular–connected UAVs depend on the cellular network and cellular infrastructure which can collapse due to a natural disaster, a viable fail–safe mechanism is needed. Other challenges, such as down–tilted base station antennas, neighboring cell interference, handover performance, multiple access, UAV mobility and link security, also need to be addressed thoroughly before the widespread implementation of a UAV network connected to the cellular networks. This has motivated several mobile operators, telecommunication vendors and research organizations to further scrutinize the propagation channel characteristics between a cellular base station and UAV. For example, Qualcomm Technologies has launched field measurements in San Diego, California, to assess the LTE network performance in a low altitude platform using a quadcopter UAV [72]. In another example [73], Ericsson and China Mobile have conducted measurement trials in China's Jiangsu province to develop a 5G prototype enabled by drone UAVs. However, these studies mainly focused on network planning and did not present any findings on the channel modeling.

In [62], a measurement campaign was launched in urban and rural scenarios in Germany to characterize the propagation channel between UAV and a cellular base station, using 900 MHz GSM network and 1.9–2.2 GHz UMTS services. Field measurements were carried out with a fixed–wing UAV and a captive balloon at altitudes up to 500 m. This work evaluated the overall RF coverage in terms of received signal strength for aerial users from the various ground base stations during the handover with regards to UAV altitude. To this end, the authors proposed an altitude–dependent channel model with the assumption that the attenuation was independent of frequency and distance. It was found that the handover rate decreases due to signal degradation at UAV altitudes above 500 m and consequently the availability of base stations decreases. To conclude, a good RF coverage was achieved for UAV altitudes upto 500 m in a rural environment. It was less due to ground obstacles than in an urban terrain.

In [63] and [74], measurement campaigns were launched under the SAAS project (remote piloted semi–autonomous aerial surveillance system using terrestrial wireless networks) in an urban environment of Lisbon, Portugal to investigate the applicability of terrestrial cellular networks in UAV communication. In [63], the field trials were performed at GSM, UMTS and LTE cellular bands using a spectrum analyzer and an antenna on a meteorological balloon, deployed as the UAV platform. In this work, an empirical model was obtained for path loss attenuation in an outdoor urban scenario. The worst case scenario was reported due to the radiation pattern of the down–tilted base station antenna for a UAV altitude between 5 to 7 m. Also, the distance in 3D space and the cellular frequency were the other performance degrading factors. However, handover analysis was not studied in this scenario. Additionally, reference [74] presented a multi–UAV network architecture based on cellular and IP networks. They have assessed the network level performance with quality–of–service measurements in terms of latency and jitter. In this case, the LTE network provides the best performance without relaying, and EDGE performs worst due to the relay between the UAVs and different base stations within the proposed architecture.

In [64], the measurements campaign was performed in a rural environment with 800 MHz LTE networks and two different cellular service providers in Denmark. The authors found considerable reduction in path loss component and shadowing variation as the UAV altitude increased. Therefore, their findings show that the UAV propagation channel requires altitude–dependent parameters for channel modeling. In contrast, [65] proposed an angle–dependent channel model to characterize propagation between the cellular base station and the UAV airborne platform. However, these studies have ignored connectivity disruption issues occurred in the UAV–cellular systems due to diffraction losses and nulls in the radiation pattern of the base station's antenna. Therefore, in [66], the measurement campaign was conducted for an open area and a mock village in California, USA, with a 909 MHz cellular band. In this work, the authors proposed the compositional path loss model to account for two–ray ground reflection propagation and diffraction losses. They also identified low coverage zones in cellular–connected UAV networks for beyond LOS operations, and named this phenomena “holes in the sky”. These holes produce unexpected coverage in the connectivity–reliant UAVs and could span from 10 m to 100 m in the coverage radius. They pointed out that the primary causes were interference caused by two–ray ground reflection, diffraction losses incurred by the Fresnel zone of the propagation path, and nulls in the antenna radiation pattern. Therefore, this study concluded that for the en–route UAV, the real–time estimation of the propagation conditions based on the geometrical information of the environment could mitigate glitches in the coverage zones of the cellular–connected UAV networks.

These measurement campaigns have mainly studied the performance of the cellular–enabled UAV network with regard to path loss attenuation. However, they did not consider the consequence of co–channel interference and did not provide in–depth handover analysis. Furthermore, the characterization of AG propagation with respect to small–scale variations and fading channel distributions were mostly overlooked. Cellular networks are not designed to provide AG propagation above the base station height due to the down–tilted sector antennas which can hinder wireless connectivity and cause significant reduction in reliability and capacity for aerial users. Therefore, optimum placement of the UAV in space and 3D features of the base station’s antenna radiation patterns should be taken into consideration for channel modeling and network planning of UAV–enabled cellular systems. Also, UAV applications such as search and rescue services and disaster management may suffer from infrastructure failure. In this case, aerial heterogeneous networks can be a promising fail–safe framework for enabling coexistence between terrestrial communication networks and satellite systems. In addition, multi–tier UAV–cellular networks as suggested in [75], can be a viable solution for avoiding traffic congestion and to restore communication services in disaster areas.

In this section, we have reviewed the measurement campaigns using UAVs as low altitude platforms. However, in these cases, channel characteristics are mostly studied with hovering or mobile UAVs and static ground users. As a result, channel dynamics may change slowly with approximately constant statistics. Also, measurement scenarios are limited to urban, suburban and rural environment with better propagation conditions. Therefore, more measurement campaigns are required in more diverse scenarios, such as metropolitan areas with skyscrapers and over water bodies. In Table I, we summarize the aforementioned measurement campaigns.

III. Empirical Channel Models from Measurement Campaigns

Channel parameters can change frequently with time and space due to the cruising capability of UAVs. Many measurement campaigns have been performed to corroborate connections between channel parameters and experimental setups. Despite of all these efforts, there are no unified answers, and conclusions still need to be established using reliable channel models. In this section we review the empirical models that characterize AA and AG propagation channels.

A. Air–to–Air (AA) Channel Characterization

The AA propagation channel is an important aspect of inter–UAV communications and can be exploited in applications, such as aerial wireless sensor networks[56], multi–UAV networks or UAV swarms[69], flying ad–hoc networks[76] and wireless back–haul connections using emerging technologies [77],[78]. In all these application, characteristics of the AA propagation depend mostly on the environmental conditions, UAV flight direction, LOS alignment, relative velocities and ground reflections. Very few empirical studies have been conducted to characterize AA channels. For instance, in [54]-[56], the AA channel was shown to be better than the AG channel in terms of path loss exponent (PLE). In [54], the authors found that the ground–to–ground (GG) channel performed poorly with a PLE of 3.57, while PLE for AA and AG channels were estimated to be 1.92 and 2.13, respectively. Similarly, in [55], the PLE was estimated from the log–distance propagation model as 0.93 and 1.50 for AA and AG propagation, respectively. On the other hand, the authors of [56] have observed that the received signal strength for AG, AA and ground–to–air (GA) propagation improves with extended UAV altitude and deteriorates as UAV distance increases. They observed that the AA channel followed two–ray propagation with a PLE of 2.05. Whereas, the presence of communication gray zones leads to asymmetry in AG and GA channels and PLEs of 2.32 and 2.51, respectively.

Aerial link characterization has been conducted in [57] and [59] using a IEEE 802.11 radio. In [57], the impact of the UAV altitude on AA propagation was investigated for large–scale variations and small–scale fading distribution. In this study, path loss was determined by the Friis equation with a PLE of 2.6 and a fading channel distribution that fits with the height–dependent Rician factor K. In [59], a log–distance model was used to analyze the path loss for vertical and horizontal distances. In this work, the minimum mean squared error (MMSE) method was utilized to compute PLEs of 2.03 and 2.01 for the AA and AG channels, respectively.

Although UAVs are placed in a 3D environment in real multi–UAV applications, the existing studies only considered the behavior of the AA propagation in a 2D plane. Moreover, these campaigns were conducted for short–range communication in an interference–limited environment. The impact of the frequency variance due to Doppler shift on the capacity and reliability of AA propagation is still unexplored. The AA channel characterization highlights that the propagation conditions are highly time–varying due to variations in the communication distance, altitude and UAV mobility. Also, significant attenuation occurs outside the LOS condition and under this scenario it may be difficult to maintain continuous connectivity for long range communication. Therefore,

TABLE I
SUMMARY OF MEASUREMENT CAMPAIGNS

Ref.	Frequency	UAV	Scenario	Altitude	Channel Statistics
[41]	2 GHz	Airship	Urban	100-170 m	RSS, PDF, CDF, AFD, LCR, PSD, AF
[42]	2 GHz	Airship	Urban	150-300 m	PL
[43],[44]	2 GHz	Airship	Urban, wooded	100-170 m	RSS, CDF, DG, AFD, LCR
[45]	5.76 GHz, 1.817 GHz	Hexacopter	Suburban	0-50 m	PL, SF, K, PDP, RMS, CDF
[46]	2.585 GHz	Hexacopter	Suburban	0-300 m	PDP, K, RMS, CDF
[47]	4.3 GHz	Quadcopter	Open field, Suburban	4-16 m	PL, SF, μ, ξ, TOA, PDP, CDF, RMS, BC
[48]	5.8 GHz	Octocopter	Residential, mountainous	–	RMS, DS, CDF
[57]	2.4 GHz	Hexacopter	Laboratory, outdoor	10-40 m	PL, PAS, K, PDF
[58]	802.11a	Quadcopter	Open field, campus area	20-100 m	RSS, PL, UDP
[59]	802.11a	Quadcopter	Open field	15-110 m	RSS, PL, PAS, UDP, CDF
[60]	802.11a	Fixed–wing	Airfield	~46 m	Pr, RSS, UDP
[61]	802.11a/g, 900 MHz	Fixed–wing	Airfield, Rural	~46 m, ~107-274 m	Pr
[62]	GSM, UMTS	Fixed–wing, captive balloon	Urban, rural	0-500 m	RSS, HO
[63]	GSM, UMTS, LTE	Weather balloon	Urban	18 m	Pr
[64]	LTE (800 MHz)	Hexacopter	Rural	15-100 m	PL, SF
[65]	LTE (850 MHz)	Quadcopter	Suburban	15-120 m	PL, SF
[66]	909 MHz	Quadcopter	Open field, mock village	40-60 m	PL, PES
[67]	802.11 b/g	Fixed–wing	Farmland	75 m	PAS, PLR, PRR, AF, DG
[72]	PCS, AWS, 700 MHz	Quadcopter	Mixed suburban	122 m	PL, RSRP, RSRQ, HO, CDF
[74]	EDGE, HSPA+, LTE	Hexacopter	-	10-100 m	Pr, RTT, J

AF: correlation function, AFD: average fade duration, BC: coherence bandwidth, CDF: cumulative distribution function, DG: diversity gain, DS: Doppler-spread, HO: handover analysis, J: jitters, K: Rician factor, LCR: level crossing rate, PAS: power azimuth spectrum, PDF: probability density function, PDP: power delay profile, PES: power elevation spectrum, PL: path loss, RMS: RMS delay spread, PRR: packet reception rate, Pr: received power, PRR: packet-loss rate, RSS: received signal strength, RSRP: reference signal received power, RSRQ: reference signal received quality, RTT: round trip time, SF: shadow-fading, TOA: time of arrival, μ, ξ: mean and standard deviation of Nakagami–m factor, UDP: UDP throughput

these open research issues need to be addressed to improve scalability and adaptability of the AA propagation channel in multi–UAV systems. Large–scale fading statistics of the AA channel are summarized in Table II.

B. Air–to–Ground (AG) Channel Characterization

1) Large–Scale Fading Statistics: Most of the AG channel measurements focus on large–scale statistics such as path loss and shadowing. For the urban environment in [42], the measured results showed that the path loss follows a distance–independent trend and is significantly affected by a low elevation angle. For the suburban environment in [45], the impact of UAV altitude and distance on the path loss was analyzed. For a vertical UAV en–route, a simplified dual slope path loss model was considered and it was found that the PLE is negative below a breakpoint altitude because of a partially cleared first Fresnel zone. When the UAV altitude increases above the breakpoint level the path loss is similar to free space propagation because the first Fresnel zone was cleared. In [47], the effect of UAV altitude and the optimal placement of the ground receiver for path loss was stochastically modeled for both static and mobile UAVs in both open field and suburban scenarios. Foliage losses and Doppler frequency shift were taken into account. In addition, shadow fading was modeled with a zero–mean Gaussian distribution and analyzed using a PDF. A further empirical study was conducted in [49], to evaluate the influence of distance on path loss attenuation, and found degraded performance of the AG channel due to detrimental effect of interference from the 802.11 devices operating in the surrounding test area. Moreover, in [50], received signal strength declined with the distance and followed the Friis channel model. In [51], the AG propagation channel in the single–hop UAV system followed the log–distance model, where higher throughput was attained over longer distance.

For an open field and a campus environment in [58], path loss was evaluated with the free space model. In [60] and [61], PLE was estimated using linear regression. In [62], distance and frequency independent empirical path loss model was proposed for urban and rural terrains, where the altitude of aerial mobile station was accounted as the key parameter. In contrast, the empirical propagation model in [63] suggested that path loss model is dependent on the distance in 3D plane and the operating frequency. In this case, other modeling parameters, such as the UAV altitude and the tilt angle of base station sector antenna, were also considered. The altitude–dependent path loss model was proposed in [64], where path loss and shadow fading decreased as the UAV altitude increased from 15 to 120 m and at about 100 m the propagation condition matched with that of free space. Conversely, in [65], the angle–dependent AG propagation channel model was

TABLE II
LARGE–SCALE FADING STATISTICS FOR AA CHANNEL

Ref.	PL model
[54]-[56]	$PL(dB) = 10\alpha\log_{10}(d)$, α =1.922[54], α =0.93[55], α =2.05[56]
[57]	$RSS(dB) = P_t + G_{UAV_1} + G_{UAV_2} + 10\log_{10}(\frac{\lambda}{4\pi d})^{\alpha}$, P_t =20 dBm, $G_{UAV_1} = G_{UAV_2}$ = 5 dBi, α = 2.6, f_c =2.4 GHz
[59]	$PL(dB) = PL(d_0) + 10\alpha\log_{10}(\frac{d}{d_0})$, $d = \sqrt{d_h^2 + d_v^2}$, $PL(d_0)$ = 46.4 dB, α =2.03, $d_h \in \{0, \cdots, 100 \text{ m}\}$, d_v = 50 m, d_0 = 1 m
α: path loss exponent, RSS: received signal strength, d: separation distance, d_0: reference distance, d_h: horizontal distance, d_v: vertical distance, G_{UAV}: UAV antenna gain	

presented, which encompasses excess path loss attenuation and shadow fading model. In this work, the model parameters are dependent on the angle between cellular base station and airborne UAV. In [66], the combinational model was developed to determine the low coverage zones in the cellular–connected UAV network. This model identified causes, such as two–ray ground reflections, diffraction losses and nulls in antenna radiation pattern as the predominant factors for path loss. The analytical path loss model was used in [72] to evaluate the performance of LTE network with UAV platform, where most of the path loss samples computed by measurements were lumped between the reference PLE of 2.0 and 4.0.

Path loss and shadowing statistics for the AG propagation channel presented in this section demonstrated that the UAV flight dynamics, such as the altitude, distance and elevation angle, are the dominant contributors for the large–scale fading. Therefore, the development of realistic UAV propagation model requires these parameters be considered in 3D coordinates. Also, considerable attention is needed for characterizing antenna design and orientations, as this will further improve UAV communications. In Table III, we summarize the large–scale fading statistics for the AG channel.

2) Small–Scale Fading Statistics: Fading amplitude statistics are important for the analysis of the small–scale variations in multipath propagation using the first order statistics, such as cumulative distribution function (CDF) and probability density function (PDF), to study the random behavior of fading channels. Also, second order statistics, such as level crossing rate (LCR), average fade duration (AFD) and fade depth (FD), are useful to analyze the severity of fading due to the spatial–temporal variations. In this subsection, several commonly used models for UAV communication small–scale fading distributions are discussed.

Loo Model is a composite channel model which accounts for Rician and Log–normal distributions. To this end, LOS component is modeled by the log–normal distribution and multipath components usually tends to follow the Rician model. In [41], the fading statistics were studied for the narrowband AG propagation channel in urban areas using the Loo model. In this case, the statistical analysis of CDF found that the empirical data fits with the simulated time series.

Rayleigh Model is well known in scattering environment. This scenario was theoretically tested for cooperative relay based UAV systems in [79]. Also, analytical study in [80] suggested that multiple–access GA channel can be modeled with the Rayleigh distribution for the UAV heading. Furthermore, the study in [39] found that the CDF of the AG propagation fading channel follows Rayleigh distribution for the field measurements with large elevation angles in a mixed–urban environment.

Rician Model is used to approximate the fluctuations in the fading channel with LOS. In the literature, this case is appropriate for the high altitude platform in [13]-[15],[26],[29],[39] and for the scattered multipath environments in the low altitude platform in [45],[46],[57]. For the Rician channel, the Rician K factor is a quantitative parameter to measure the severity of the multipath fading. In [45], the variations in the received signal amplitude for the AG propagation was found as K=5.29 dB for ascending and descending directions of the UAV altitude and K up to 19.14 dB for horizontal flight trials in two different zones at the altitudes of 20 m and 30 m. On one hand, for the AG propagation, [46] proposed Rician K as a piece–wise function of the altitude with a break–point of 16 m. On the other hand, the AA channel characterization in [57], studied the influence of the altitude–dependent Rician K due to scattered ground reflections and found that, as UAV elevated from 10 m to 40 m, the value of K increases from 3.533 to 10.048 dB. This work indicated that the impact of the ground reflected multipath fading reduces with increasing UAV altitude. Theoretical implication of Rician fading channels was found in [17] to improve MIMO gain for AG propagation in a hilly rural scenario and in [81], when combined with two–state Markov model to capture channel non–stationarity.

Nakagami–m and Weibull fading models are appropriate for characterizing the UAV fading channels intended for high altitude applications [79]. Rayleigh channel distribution is a special case of Nakagami–m. In [47], magnitudes of individual multipath components were collected for different time delay bins and modeled by the Nakagami–m distribution. In this case, mean and standard deviation of the m parameter were empirically estimated. As a result, the mean was found to be small for both open and suburban areas under the influence of vegetation, and large variance was observed due to thick suburban scattering. Furthermore, in [59], the CDF analysis found that the Nakagami–m distribution fits the empirical data better compared with Rayleigh distribution. Both Nakagami–m and Weibull fading distributions can offer substantial flexibility to study the UAV fading channel characteristics in diverse environment. However, empirical studies have not yet been initiated for development of statistical channel model based on Weibull distribution, as for vehicle–to–vehicle channel modeling [82].

TABLE III
LARGE–SCALE FADING STATISTICS FOR AG CHANNEL

Ref.	PL model
[42]	$PL(dB) = -10\log_{10}[\frac{0.05\lambda}{2h^2}(d_{2d} + r_b^2 d_{2r})] - 20\log_{10}(1 - e^{\varrho})^2$, $\varrho = -0.6038\times 0.109^{\nu}$, $\nu \approx h\sqrt{\frac{2}{\lambda d_2}}$, h: obstruction height, d_2: distance between receiver and obstruction, d_{2d}: direct–ray distance between receiver and obstruction, d_{2r}: reflected–ray distance between receiver and obstruction, r_b: reflection coefficient
[45]	Vertical: $$PL(dB) = \begin{cases} PL(d_0) + 10\alpha_1(\log_{10}\frac{d}{d_0}) & \text{if } d < d_b, \\ PL(d_0) + 10\alpha_1(\log_{10}\frac{d}{d_0}) + 10\alpha_2(\log_{10}(\frac{d}{d_b})) & \text{if } d \geq d_b, \end{cases}$$ $(\alpha_1, \sigma_1 dB)$ = (0.74, 1.23), $(\alpha_2, \sigma_2 dB)$ = (2.29, 2.15), d_b = 9 m Horizontal: $PL(dB) = PL(d_0) + 10\alpha(\log_{10}\frac{d}{d_0})$, for 20 m: $(\alpha, \sigma dB, PL(d_0)dB)$ = (0.93, 5.5, 77.9), for 30 m: $(\alpha, \sigma dB, PL(d_0)dB)$ = (1.01, 3.9, 74.6)
[47]	Static UAV: $PL(dB) = PL(d_0) + 10\alpha(\log_{10}\frac{d}{d_0}) - \log_{10}\frac{\triangle h}{h_{opt}} + C_p + \zeta$, $\triangle h = \|h_g - h_{opt}\|$, $\triangle f = (\frac{\triangle v}{c})\cdot f_c$, $\zeta \sim N(0, \sigma^2)$, C_p = 0 dB, d = 5.6 m to 16.5 m, h_g = (1.5 m, 7 cm), $(\alpha, \sigma dB, PL(d_0)dB)$ = 2.6471, 3.37, 34.905 (open, 0 km/h), $(\alpha, \sigma dB, PL(d_0)dB)$ = 2.7601, 4.8739, 30.4459 (suburban, 0 km/h), Mobile UAV: $PL(dB) = PL(d_0) + 10\alpha(\log_{10}\frac{d}{d_0}) - \log_{10}\frac{\triangle h}{h_{opt}} + C_p + 10x\log_{10}(\frac{f_c + \triangle f}{f_c}) + \zeta$, $(\alpha, \sigma dB, PL(d_0)dB)$ = 2.6533, 4.02, 34.906 (open, 32 km/h), $(\alpha, \sigma dB, PL(d_0)dB)$ = 2.8350, 5.3, 30.446 (suburban, 32 km/h), x: frequency dependent path loss factor and negligible at small velocities
[49]	$RSS(dBm) = -95 + 10\log_{10}(K_0 . d^{-\alpha})$, α = 2.34, $K_0 = 3.6\times 10^{-1}$
[50]	$RSS(dB) = P_t + G + 10\log_{10}(\frac{\lambda}{4\pi d})^{\alpha}$, P_t = 20 dBm, G = 1dB, f_c = 2.4 GHz, α = 2.3
[51]	$PL(dB) = 10\alpha\log_{10}(d)$, $\alpha \approx$2 for beyond 100 m distance
[54]-[56]	$PL(dB) = 10\alpha\log_{10}(d)$, α = 2.132 (AG), 3.57 (GG)[54], 1.50 (AG)[55], 2.32 (AG), 2.51 (GA), 3.1 (GG)[56]
[59]	$PL(dB) = PL(d_0) + 10\alpha\log_{10}(\frac{d}{d_0})$, $d = \sqrt{d_h^2 + d_v^2}$, $PL(d_0)$ = 46.4 dB, α = 2.01 (AG), $d_h \in \{0, \cdots, 100 \text{ m}\}$, d_v = 50 m, d_0 = 1 m
[58]	$RSS(dBm) = P_{rx}(d_0) - 10\alpha\log_{10}(\frac{d}{d_0})$, α = 2.2 (open), 2.5-2.6 (campus), P_{rx}: received power at reference distance
[60],[61]	$RSS(dBm) = A - 10\alpha log_{10}(d)$, (α, A) = (1.80, -37.5)[60], (α, A) = (1.04, -55.12)[61]
[62]	Urban: $PL(dBm) = 89.5357 + (\frac{h_{UAV}^3}{10000} + 0.0108h_{UAV}^2 + 0.8588h_{UAV})$ Rural: $PL(dBm) = 78.2186 - 0.0013h_{UAV}^2 - 0.0052h_{UAV}$, $h_{UAV} \in \{0, \cdots, 500 \text{ m}\}$
[63]	$PL(dB) = 20\log(\frac{4\pi d_0}{\lambda}) + X_{dis} + X_{freq} + X_{hei} + X_{ang}$, $X_{dis}, X_{freq}, X_{hei}, X_{ang}$: 3D distance, frequency, altitude and tilt angle dependent parameters
[64]	$PL(dB) = \alpha(h_{UAV})10\log_{10}(d) + \beta(h_{UAV}) + \zeta$, $\zeta \sim N(0, \sigma(h_{UAV}))$, for h_{UAV} = 15-100 m: $\alpha(h_{UAV})$ = 2.9-2.0, $\beta(h_{UAV})$ -1.3-35.3 dB, $\sigma(h_{UAV})$ = 7.7-3.4 dB
[65]	$PL(dB) = \alpha 10\log_{10}(d) + A(\phi - \phi_0)\exp(-\frac{\phi - \phi_0}{B}) + \eta_0 + \zeta$ $\zeta \sim N(0, a\phi + \sigma_0)$, α = 3.04, A = -23.29, B = 4.14, ϕ_0 = -3.61, η_0 = 20.70, a = -0.41, σ_0 = 5.86
[66]	$PL(dB) = -20\log_{10}\|\nu\| + 40\log_{10}(d) - 10\log_{10}(h_{BS}^2 h_{UAV}^2)$, ν: Kirchoff diffraction parameter
[72]	$PL(dB) = P_{tx} - 10\log_{10}(12.BW) - RSRP + G_{UAV} + G_{BS}$ P_{tx}: maximum transmit power, BW: transmission bandwidth, $RSRP$: measured reference signal received power, G_{UAV}: gain of UAV antenna, G_{BS}: gain of base station antenna
α: path loss exponent, RSS: received signal strength, d: separation distance, d_0: reference distance, d_b: breakpoint distance, C_P: foliage loss, σ: standard deviation, h_g: height from ground level, h_{opt}= optimal height from ground level, f_c: carrier frequency, h_{UAV}: UAV altitude, h_{BS}: base station altitude, $\triangle f$: Doppler shift, K_0: transmission gain, G: antenna gain, A: y–intercept, λ: wavelength	

Doppler spread and delay dispersion, UAV channels tend to posses higher Doppler spread than the conventional radio channel because the relative velocities of UAVs are higher. In [45] and [46], delay spread resolution was in micro–seconds for suburban environment. In [47], excess delay and RMS delay spread were of the order of nano–seconds for a foliage environment. In this case, channel impulse response was obtained by Clean algorithm. However, frequency variance due to Doppler shift is not significant in [46],[47] due to the low velocity of UAVs. In [48], for the mountainous desert scenario, the median RMS delay spread and the Doppler frequency spread were roughly $0.06\mu s$ and 28.96 Hz, respectively. For the residential area, the measured median RMS delay spread and the Doppler frequency spread were approximately $0.03\mu s$ and 28.06 Hz. The RMS delay spread attained in the desert terrain was larger due to the rough mountainous scatters along the flight path than those in the residential area. In this case, RMS delay spread was modeled as log–normal distribution. However, these works lack the second order statistics, such as AFD, LCR and FD, for the spatial–temporal variations in the AG propagation channel.

Fading channel statistics for most low altitude AG propagation cases reported in the literature are analyzed with the Nakagami–m and Rician distributions. Weibull distribution is still unexplored. Also, estimation of the fading channel characteristics for the AA propagation with regards to altitude and surface scattering is an open research issue. Table IV provides the empirical fading distributions for small–scale variations with both manned aircrafts and UAVs.

IV. Analytical Channel Models

Analytical channel models are useful for characterizing the propagation behavior under certain assumptions and parameters. They can predict the performance of communication systems. For example, channel behavior of land mobile satellite systems can be analyzed using the multi–state Markov chain model [4],[5]. Generally there are three main modeling approaches: deterministic, stochastic and geometry–based stochastic approach.

A. Deterministic

In deterministic models, environmental clutters are placed in certain layouts. This approach assumes large dimensions of the environmental objects in comparison with the wavelength, it does not compensate the diffuse scattering. The accuracy of these channel models depends on the environment–specific database which consists of the information related to the terrain topography, the electrical parameters of buildings and other obstruction materials. Deterministic models can be realized by the ray–tracing software, which can depict the realistic behavior of the EM wave propagation and simulate path loss and shadowing effects.

In [6], 3D ray–tracing was performed to characterize the altitude–dependent attenuation in the AG propagation for the suburban environment. In [7] and [8], analytical propagation models have been studied for the AG channel characterization in an urban environment for frequencies ranging from 200 MHz to 5 GHz and altitudes from 100 to 2000 m. In [7], the path loss and shadowing statistics were examined as a function of elevation angle and the aerial altitude through 3D ray–tracing. The authors have provided analytical path loss expressions. Also, the shadowing was fitted with the log–normal distribution with the standard deviation dependent on the elevation angle. The work in [8] utilized knife–edge diffraction theory to model the LOS probability, which considered the statistical parameters to account for height, size and coverage area of buildings in the simulation.

In [9]–[11], environmental topography was realized with the statistical parameters recommended by the International Telecommunication Union (ITU–R). In [9], a generic path loss model for a low altitude platform was proposed, where the channel model parameters were estimated by 3D ray–tracing at 700 MHz, 2000 MHz and 5800 MHz. In this work, the AG channel conditions favoring LOS and non–LOS (NLOS) propagations were grouped distinctly and analyzed with the group occurrence probability as the conditional PDF. Simulation results demonstrated that the impact of elevation angle was significant on the excess path loss. In [10], the closed–form expression was formulated for determining the coverage performance in terms of the maximum cell radius and the optimal altitude. In this study, the free space path loss model was extended using the excessive attenuation factor for different LOS and NLOS propagation conditions. This was extended in [11] to provide the analytical framework for optimization of the average radio coverage probability and the maximum transmission rate to achieve the required quality–of–service. However, in these works, propagation conditions depend upon the altitude and coverage radius of the UAV. As the altitude increases with respect to radius, the LOS probability tends to 1 for all ground positions. Therefore, such channel model can only be appropriate for the high–rise urban environment with an average building height of 60 m. In contrast, the channel model in [83] was recommended for the modern metropolitans with densely located skyscrapers. However, this model requires more environmental data, such as shape of buildings with surrounding geometry.

The path loss model in [10] addressed the technical challenges in UAV communication, such as optimum deployment of the UAV in [11],[12], outage and bit–error rate (BER) analysis in [84], energy efficiency of UAV networks in [85]-[87], interference management in multi–UAV scenario in [88], latency in UAV–enabled cellular networks in [89] and UAV flight endurance time in [90]. Furthermore, this model complements the optimum deployment of UAVs to ensure maximum reliability in terms of the outage capacity and the BER using static and mobile aerial relays in [91]. It increases the number of users in cellular–assisted UAV network in [92] and UAV for data caching purpose in [93]. In these applications, UAV channel model incorporates both LOS and NLOS propagation conditions for a certain set of environmental parameters. Also, the appropriate placement of the UAV is of paramount importance.

These studies have suggested that deterministic UAV channel models account for the reciprocity ascertained in the propagation channel to the UAV placement and the propagation conditions in different environments. However, in [6]–[8], channel models were confined to the urban and the suburban environments and did not capture generality for other environments. Channel models in [9],[10] are applicable for environmental statistics based on ITU–R recommendations. These studies have characterized propagation channels for a static UAV and ignored the fading effects due to the small–scale variations. In contrast, studies in [45],[47],[57],[59] have empirically analyzed the variations in the received signal strength and provided large–scale and small–scale statistical properties of UAV channels. However, these works have largely overlooked the impact of environment on the propagation conditions and consequently the UAV coverage analysis. Furthermore, experimental work has not yet been conducted for UAV channel modeling in metropolitans with skyscrapers. In contrast, reference [83] provided the analytical approach and ray–tracing simulations for the AG propagation characteristics in metropolitan scenario emulated by the Manhattan grid. Therefore, more empirical and analytical studies are required to provide ubiquitous coverage using UAV networks in versatile environments and specifically for metropolitans, considering that UAVs have been envisaged as a potential candidate to support 5G mobile communication systems [94]. Some of the deterministic UAV channel models are reported in Table V.

TABLE IV
SMALL–SCALE FADING DISTRIBUTIONS

Ref.	Scenario	Frequency band	UAV channel	Fading distribution	Parameters
[13]-[15]	Over water[13], hilly[14] and suburban[15]	Wideband	AG	Rician	K ~ 20–27 dB in C band and K ~ 12 dB in L band [13], K=29.4 dB in C band and K=12.8 dB in L band [14], K=28.5 dB in C band and K=14 dB in L band [15]
[26]	Urban	Wideband	AG	Rician	K=34 dB
[29]	hilly	Wideband	AG	Rician	-
[39]	Mixed urban	Wideband	AG	Rician (for small elevation angles), angle–dependent Rayleigh (for large elevation angles)	-
[41]	Urban	Narrowband	AG	Loo model (Rician & Log-normal)	-
[45]	Suburban	Narrowband	AG	Rician	K=5.29 dB for vertical mobility 0-50 m, K=(6.57,9.74 dB) for horizontal mobility at 20 m and 30 m altitude in Zone 1, K=(13.57,19.14 dB) for horizontal mobility at 20 m and 30 m altitude in Zone 2
[46]	Suburban	Narrowband	AG	Rician	For UAV altitude of h m, $K(h)$ dB= $\begin{cases} 3.53+0.65h, & 0<h\leq 16 \\ 29.6-17.4\log_{10}h, & h>16 \end{cases}$
[47]	Open field, suburban	Ultra–Wideband	AG	Nakagami–m	-
[57]	Outdoor	IEEE 802.11	AA	Rician	K=3.533, 10.120 and 10.048, respectively, for altitudes of 10, 25 and 40 m
[59]	Open field	IEEE 802.11	AG	Nakagami–m	m=4.02 for hovering test at -62 dBm received power, m>1 for mobility at all distances

B. Stochastic Channel Model

For UAV communication, stochastic channel models can be designed using the tapped delay line (TDL) system with different numbers of taps, each of which can accommodate fading statistics of the multipath components derived from the channel impulse response. In this case, fading statistics of individual taps can be analyzed empirically from measurements and numerically by computer simulation. However, the accuracy of these model depends on the estimation of stationary interval in the non–stationary UAV channel.

In [13]-[15], wideband stochastic channel models were proposed from the data collected in different environments, using the estimated stationary interval of 15 m at the C band. For over water settings in [13], the AG channel employed the TDL model to characterize the two–ray propagation with an additional multipath component as the intermittent ray. In this work, the authors have argued that the statistics for LOS and reflected components can be analyzed either as the curved earth two–ray (CE2R) model or the flat earth two–ray (FE2R) model. The probability of the existence of the intermittent multipath component was estimated by the exponential distribution as a function of link distance. The TDL model with nine taps have been proposed for the mountainous terrain [14] and the suburban environment [15].

In [95] and [96], stochastic model was developed with the narrowband assumption to characterize the aeronautical AG channel. In [95], the stochastic model was designed for characterizing the AG propagation in terms of transmission coefficients assuming that the quadrature components reflected from the ground surface can be modeled as a zero–mean Gaussian process. Also, Doppler spectrum analysis was performed for the diffuse multipath components. In [96], the proposed model was developed with the TDL system having both LOS and NLOS taps, where the amplitude attenuation and the multipath delay of NLOS components were assumed to be Rayleigh distributed and Gaussian random process, respectively, while the phase shift was uniformly distributed. In addition, the Doppler frequency shift was characterized as a random process. However, channel stationarity interval was not computed and fading statistics were assumed to be constant for the random time duration.

Stochastic models provide useful analysis of the time–varying characteristics of the UAV channel. For instance, reference [97] proposed the TDL model to capture the small–scale characteristics of multipath components. Furthermore, the stochastic model accommodates multi–antenna system to boost the reliability of MIMO channel in terms of BER in [98] and capacity in [99]. In these works, the stochastic model only provides numerical analysis and lacks in validation by measurement results. On one hand, empirical data have been collected from the measurement campaigns in [45],[47],[48] to study the impact of UAV flight dynamics and environment on the small–scale fading. However, these studies did not consolidate the fading statistics using the TDL model. Also, estimation of the stationary interval in the UAV channel was ignored in these works. On

TABLE V
DETERMINISTIC MODELS

Ref.	Analytical Model	Parameters
[7]	Path loss: $$PL(dB) = \begin{cases} -0.58 + 0.549 e^{\frac{(90-\phi)}{24}}, & \text{LOS channel} \\ \eta_0 - \eta_1 e^{-\frac{(90-\phi)}{\nu}}, & \text{NLOS channel} \\ \iota_0 - \iota_1 e^{\frac{(90-\phi)}{\omega}}, & \text{obstructed (OLOS) channel} \end{cases}$$ Shadow fading: $\sigma(dB) = \rho(90-\theta)^{\gamma}$,	ϕ: elevation angle, for 200 MHz: (η_0, η_1, ν)= (9.08, 6.40, 12.01), (ι_0, ι_1, ω)= (2.11, 0.41, 22.07), for 5000 MHz: (η_0, η_1, ν)= (20.43, 14.60, 10.50), (ι_0, ι_1, ω)= (6.23, 0.4787, 22.65), LOS channel at 200 MHz and 100 m altitude: (ρ, γ)= (0.0143, 0.9941), NLOS channel at 200 MHz and 5000 MHz: (ρ, γ)= (0.7489, 0.4638) & (2.7940, 0.2259), OLOS channel at 200 MHz and 5000 MHz: (ρ, γ)= (0.3334, 0.3967) and (0.8937, 0.3713)
[8]	LOS probability in a street: $$P_{LOS} = \begin{cases} 1 - \frac{S_c \sin\vartheta}{W_s}, & 0 < S_c < W_s/\sin\vartheta \\ 0, & S_c > W_s/\sin\vartheta \end{cases}$$ LOS probability in an area: $P_{LOS} = \frac{2}{\pi}[\vartheta_c - \frac{S_c(1-\cos\vartheta_c)}{W_e}]$,	ϕ: elevation angle, ϑ: street angle, ϑ_c: critical street angle, W_s: street width, S_c: critical distance between ground station to adjacent buildings, H: building height, h_g: ground station height, W_e: estimated street width, λ: wavelength, W_s = 15 m, $\vartheta = 90°$, $\Delta H = H - h_g$, H = 11.71 m, h_g = 15 m, W_e = 44.2 m $$S_c > \Delta H \cot\phi + \frac{0.16\lambda\cos\phi + \sqrt{(0.16\lambda\cos\phi)^2 + 0.32\lambda\Delta H \sin\phi}}{\sin^2\phi},$$ $$\sin\vartheta_c = \begin{cases} \frac{W_e}{S_c}, & W_e \leq S_c \\ 0, & \text{otherwise} \end{cases}$$
[9]	Path loss: $PL(dB) = 20\log(\frac{\triangle h}{\sin\phi}) + 20\log(f_{MHz}) - 27.55$, LOS probability: $P_{LOS} = a(\phi - \phi_0)^b$,	h_{UAV}: UAV altitude, $\triangle h = h_{UAV} - h_g$, h_{UAV} = 200 m, h_g = 1.5 m, f_{MHz} = 700, 2000, 5800, $\phi_0 = 15°$, For 700 MHz: suburban(a = 0.77, b = 0.05), urban(a = 0.63, b = 0.09), dense urban(a = 0.37, b = 0.21), high–rise urban(a = 0.06, b = 0.58)
[10]	Path loss: $PL(dB) = \frac{\varepsilon_{LOS} - \varepsilon_{NLOS}}{1 + A\exp(-B[\arctan(\frac{h_{UAV}}{r}) - A])} + 10\log d + 20\log(\frac{4\pi f_c}{c}) + \varepsilon_{NLOS}$,	$d = (h_{UAV}^2 + r^2)$, r: coverage radius, c: speed of light, For $f_c = 2000 MHz$: suburban($\varepsilon_{LOS}, \varepsilon_{NLOS}, A, B$) = (0.1, 21, 4.88, 0.43), urban($\varepsilon_{LOS}, \varepsilon_{NLOS}, A, B$) = (1, 20, 9.61, 0.16), dense urban($\varepsilon_{LOS}, \varepsilon_{NLOS}, A, B$) = (1.6, 23, 12.08, 0.11), high–rise urban($\varepsilon_{LOS}, \varepsilon_{NLOS}, A, B$) = (2.3, 34, 27.23, 0.08)

the other hand, [13]-[15] did estimate the stationary interval in stochastic TDL models for different operating environments. However, these campaigns were conducted using manned aircraft at high altitude. Therefore, the effective stochastic framework has to be developed for UAV channels in low altitude which also accommodates channel non–stationarity. In Table VI, we have presented the channel response from the TDL models reported in this paper.

C. Geometry–based Stochastic Channel Model

Geometry–based stochastic modeling approach obtains the spatial–temporal channel characteristics with the stochastic output in a 3D geometric simulated environment. The accuracy of this model is dependent on the simulation of the virtual environment confined in some geometrical shapes, such as cylindrical or elliptical where communication nodes within scattering region follow a certain probability distribution. The geometric based channel model for the analysis and simulation of the AG radio communication was proposed in [16]. It characterized the multipath propagation in a cluttered environment around the ground station confined within a virtual 3D ellipsoidal geometry to analytically evaluate delay, gain, phase and angle of arrival (AOA) of individual multipath components. In addition, path loss model may be determined using the log–distance model between the airborne platform and the clutters. Therefore, the proposed model is equally applicable to determine both narrowband and wideband channel statistics and well suited for designing antenna diversity system and antenna arrays. This work was extended in [17] for theoretical estimation of the MIMO performance for the low altitude AG propagation and also characterized the propagation loss for LOS and multipath components using the log–distance path loss model with log–normal shadowing. In this model, the small–scale fading due to spatial variations was modeled by the Rician distribution to analyze the severity of the fading due to the scattering phenomenon. Furthermore, the probability of error was simulated for single–input single–output (SISO) system and compared with a 2×2 space–time block coding and a 2×2 spatial multiplexing gain using maximum likelihood detection. In [18], a 3D AG propagation model was proposed for the dense scattering environment considering low altitude platform. The model was derived for a direction of arrival and the delay dependent Doppler spectrum with the approximation of linear distribution of the scattering point. In this work, the analytical results were compared with the simulation results by using the terrain based digital elevation model and found that the terrain morphology affects the Doppler–delay spread spectrum.

In [19], a realistic 3D geometric–based stochastic model has been developed for the AG communication between an airborne platform and the base station as an elevated plane. The proposed model considered scattering points as uniformly distributed around the base station. In this study, the spatial characteristics were analyzed with the closed–form analytical expressions. In [20], the geometric–based stochastic approach has been utilized for UAV channel modeling to analytically characterize a 2×2 MIMO enabled AG propagation in a 3D plane. In this case, the model was developed with the assump-

TABLE VI
TDL MODELS

Ref.	TDL model
[13]	$h(\tau,t) = h_{2-ray}(\tau,t) + w_3(t)A_3(t)\exp(-j\varphi_3(t))\delta(\tau-\tau_3(t))$, h_{2-ray} denotes FE2R or CE2R model, $w_3(t) \in \{1,0\}$ represents presence/absence of the intermittent ray and modeled as $p(d) = ae^{bd}$, A_3 is the amplitude of the intermittent ray and modeled by the Gaussian distribution, $\varphi_3 \in \{0,2\pi\}$ is the uniformly distributed phase of the intermittent ray, τ_3 is the excess delay of the intermittent ray and modeled as $p(\tau_3) = \frac{1}{\mu}e^{-(\tau_3-100/\mu)}$, (a,b) = (0.17,-0.25) over sea water and (0.03,-0.15) over freshwater, μ= 17 ns, 6 ns $\leq \tau_3 \leq$ 7 ns, d: link distance
[14], [15]	$h(\tau,t) = A_1(t)\delta(\tau-\tau_1(t)) + A_2(t)\exp(-j\varphi_2(t))\delta(\tau-\tau_2(t)) + \sum_{L=3}^{9} w_L(t)A_L(t)\exp(-j\varphi_L(t))\delta(\tau-\tau_L(t))$, A, φ and τ denotes amplitude, phase and excess delay, respectively, subscripts 1, 2 and L represents LOS, reflected and L^{th} intermittent multipath components, respectively, variations of w_L and τ_L are modeled as a linear function of link range, $\varphi_L \in \{0,2\pi\}$ is the uniformly distributed phase, $10\log\left(\frac{A_L^2}{A_1^2}\right)$ represents relative power of intermittent components and follows a Gaussian distribution
[96]	$y(t) = A_1(t)\cos[2\pi\{f_c+\triangle f\}(t-\tau_1(t))] + \sum_{L=2}^{N} A_L(t)\cos[2\pi\{f_c+\triangle f\}(t-\tau_L(t)) + \varphi_L(t)] + n(t)$, A_1 is the amplitude of LOS path, A_L represents amplitude of NLOS paths and assumed as Rayleigh random process, $\varphi_L \in \{-\pi,\pi\}$ is the phase shift of NLOS paths and modeled as the uniform random process, $\triangle f$ denotes Doppler frequency shift and modeled as time–variant random process, τ_1 = 25 μs, τ_L is excess delay of NLOS components and modeled as the Gaussian random process with mean and standard deviation of 30 μs and 5 μs, respectively, $n(t)$ is white Gaussian noise

tion that the ground scatters were distributed on the cylindrical surface and scatter free airborne environment. Based on the proposed model, analytical expressions were used to study the impact of the elevation angle and the direction of the UAV movement on the space–time correlation function in a non–isotropic environment.

While deterministic and stochastic models can provide useful understanding of the propagation characteristics in the UAV communication, these models are usually not feasible with a large number of simulation parameters. Geometry–based stochastic channel model emerged as a preferable method to derive analytical expressions for the predominant performance metrics. The practicability of such model is to predict coverage and capacity performance. For instance, in [100], extended coverage and enhanced capacity has been achieved by concurrency between a single UAV and device–to–device users distributed as a Poisson point process. Furthermore, downlink coverage analysis has been performed in [21] for the multiple UAVs modeled as a uniform binomial point process at the fixed altitude and a single ground user. Also, in [101], the network planning approach has been developed based on the stochastic geometry. In these studies, ground users were spatially positioned with a uniform distribution. However, more realistic UAV channel model based on the stochastic geometry framework can accommodate non–uniform distribution for both UAVs and ground users and therefore, can be considered as the future research direction in this domain. Implications of the geometric–based stochastic approach is to model the channel non–stationarity, to get insights of the angular information for multipath components in scattering regions [16],[19],[20], and for joint Doppler–delay spectrum [18]. However, these studies are largely simulation based. Therefore, the empirical framework has to be developed to characterize propagation with regard to spatial–temporal variations in the non–stationary UAV channels. Some analytical expressions to determine AOA using geometry–based model are given in Table VII. Finally, pros and cons of different UAV channel modeling approaches are enlisted in Table VIII.

V. IMPORTANT ISSUES

A. Airframe Shadowing

In UAV communication, the radio path between aircraft and ground control station may be blocked by aircraft structure, such as wings, fuselage or engine. Also, during flight maneuvering or banking turns, the direct LOS path may be severed and thus, induce shadowing. In the case of small size UAVs, airframe shadowing may occur due to different types of UAVs, such as multi–rotors, sharp transitions in flight dynamics, aerodynamics due to structural design, type and placement of on–board antenna and material. In the context of UAV channel characterization, airframe shadowing is still unexplored, as most of the measurement campaigns pertinent to this phenomena are initiated with manned aircrafts in high altitude. Therefore, the characterization of airframe shadowing with multi–rotor UAVs in low altitude is an interesting topic. For manned aircrafts, in [26], channel measurements were extracted for the communication link between aircraft and satellite. Characterization of the AG channel in the C band was performed in [27]. Reference [28] analyzed the CDF of the received signal power during the circular flight track. In [29], airframe shadowing was reported due to wings and engine of the commercial A320 aircraft. Empirical airframe shadowing model was proposed in [30].

B. Stationary Interval

One of the most important characteristics that distinguish UAV communication from the conventional communication is the non–stationarity in UAV channels, where the WSSUS assumption is violated. Therefore, wideband frequency–dispersive channel statistics are important within the stationary interval of the non–stationary UAV channel. No comprehensive study is available in the literature that addresses non–stationarity for the UAV propagation channel in low altitude platform. Therefore, estimation of the stationary interval is a contemporary research topic. Efforts to characterize the AG channel with stationarity interval were made in [71]. In this study, stationary interval was computed

TABLE VII
GEOMETRY–BASED STOCHASTIC MODEL

Ref.	Geometry–based stochastic model
[16]	The PDF of AOA as a function of elevation angle (ϕ) around the ground receiver: $f(\phi) = \frac{\frac{x_a^2}{x_a^2 - x_b^2} - 1}{2\pi\gamma\left(\frac{x_a}{\sqrt{x_a^2 - x_b^2}} - \cos\phi\right)^2}$, where x_a and x_b are subsequently the major and minor axis of the planar elliptical scattering surface, $\gamma = \frac{x_a}{\sqrt{x_a^2 - x_b^2}}\left(\frac{x_a^2}{x_a^2 - x_b^2} - 1\right)^{\frac{1}{2}}$
[19]	The PDF of AOA with respect to airborne platform: $f(\Psi_{ap}, \phi_{ap}) = \frac{\left(l_{ap,max}^3 - l_{ap,min}^3\right)\cos\phi_{ap}}{3V}$, where Ψ_{ap} and ϕ_{ap} are, respectively, the azimuth and the elevation angle observed from the airborne platform, $l_{ap,max}$ and $l_{ap,min}$ are the distance between the UAV and, respectively, the farthest and the nearest scatter point The PDF of AOA with respect to the elevated ground plane: $f(\Psi_{bs}, \phi_{bs}) = \frac{\left(l_{bs,max}^3 - l_{bs,min}^3\right)\cos\phi_{bs}}{3V}$, where Ψ_{bs} and ϕ_{bs} are, respectively, the azimuth and the elevation angle observed from the base station, $l_{bs,max}$ and $l_{bs,min}$ are the distance between the base station and, respectively, the farthest and the nearest scatterer point, and V is the volume of the scattering region
[20]	The von Mises PDF of AOA as a function of azimuth angle: $f(\Psi) = \frac{e^{k\cos(\Psi - \Psi_\mu)}}{2\pi I_0(k)}, -\pi < \Psi \leq \pi$, where k is a spreading control parameter, $\Psi_\mu \in [-\pi, \pi]$ is the mean angle of the distribution of scatterers in a 2D plane, $I_0(.)$ is the zeroth–order modified Bessel function, k=3, Ψ_μ=π, The cosine PDF of AOA as the function of elevation angle: $f(\phi) = \frac{\pi}{4\phi_m}\cos(\frac{\pi}{2}\frac{\phi - \phi_\mu}{\phi_m})$, with mean angle $\phi_\mu = \frac{\pi}{6}$ and variance $\phi_m = \frac{\pi}{4}$

TABLE VIII
PROS AND CONS OF CHANNEL MODELING APPROACHES

Modeling approaches	Pros	Cons
Empirical	• Large–scale fading can be analyzed by linear regression technique [60]-[61] and curve fitting [62] applied on the received signal strength • Path loss model presented as closed–form expressions with correction factors based on environment conditions [47], UAV altitude [62],[64] and elevation angle [65] • Small–scale fading can be characterized by the superposition of all multipath components in the form of channel impulse response [45]-[48] • Channel characterization is possible for the AA propagation [54]-[57],[59] with different UAV flight dynamics and velocities	• Tedious and expensive measurement campaigns • Channel characterization depends upon the multipath resolution of the channel sounder, antenna design and propagation environment • Size and payload constraints of different UAV types • Restrictions on UAV flight altitude by national civil aviation regulatory authorities [23]-[25]
Deterministic	• Reliable characterization of the AG propagation for large–scale fading statistics [6]-[10] • Effective optimization for coverage [11]-[12], reliability [84],[91] and capacity performance in UAV communications • Often presented as closed–form expressions [6]-[10]	• Environment specific modeling approach • Require large databases of environment geometries such as shape, size and position of all obstacles [6]
Stochastic	• Low computational complexity to emulate complete UAV propagation characteristics in versatile environment [96] • Characterization of multipath components can be done with both numerical [95]-[96] and empirical analysis [13]-[15]	• Estimation of fading statistics are dependent on the stationary interval of the dynamic UAV channel
Geometry–based stochastic	• 3D channel characterization is possible with less environmental parameters to study the channel state information in UAV propagation for e.g. angular information due to spatial–temporal variations without considering non–stationarity in the UAV channel [16],[18] • Suitable for the analytical realization of UAV–MIMO channel in low altitude platform [17],[20]	• Accuracy is dependent on the distribution of scatters confined in a target area of specific shapes • High computational complexity

for the wideband measurements using temporal PDP (power delay profile) correlation coefficient method, whereas, spatial correlation collinearity was considered for the narrowband measurements. The estimated stationary interval from both of these methods were approximately 15 m or 250λ at the C band with the bandwidth of 50 MHz.

C. Diversity Gain

Diversity is beneficial to enhance the reliability of the communication systems, particularly when deep fades dominate. Terrestrial MIMO has been widely recognized to offer superior diversity gain and high spectral efficiency in rich multipath environment. However, its applicability in UAV communication is still restrained by several factors. First, the spatial multiplexing gain in the airborne MIMO is often hindered by the lack of scattering environment near UAVs, which could only provide minimal throughput improvement in comparison with the single antenna UAV systems. Second, it might be difficult for small size UAVs to accommodate multiple antennas or antenna array with large inter–element distance to improve spatial multiplexing gain. However, smaller carrier wavelength can make it feasible to mount small antenna array, but at the expense of higher path loss. Furthermore, power consumption by the multiple antenna system places major constraint to battery operated UAVs. Moreover, UAV–MIMO gain can be further curtailed due to difficulty in acquiring accurate channel state information for a highly time–variant AG channel. Despite these challenges, some studies have exploited MIMO technology in the airborne environment. For example, in [31], a 4×4 MIMO enabled OFDM system was used to increase the average throughput by 2 times and the range extension by 1.6 times in comparison to a SISO system. In [32], multiple helicopter mounted antennas were utilized to achieve the signal–to–noise (SNR) gain of approximately 13 dB. In [34], the spatial multiplexing gain was achieved with a 2×2 MIMO configuration and consequently enhanced the throughput gain up to 8 times for most of the flight route. However, these studies are conducted with manned aircrafts in the high altitude platform. For UAV communications, there are very few measurement campaigns on the effect of multiple antenna systems. In [43] and [44], the AG channel characterization was initiated with a 1×4 antenna configuration. In this work, carrier–to–noise ratio (CNR) gain was compared for the common combining strategies such as selection, equal–gain and maximal ratio combining (MRC). In [67], the performance of multiple receiver and transmitter nodes was evaluated by the correlation coefficient. In this case, the packet delivery rate was boosted by 25% on average due to the poor correlation at the multiple receiver nodes in a 1×4 configuration and by 37% with the selection diversity using three transmitters in a 3×4 setup. Measurement of a 4×4 MIMO channel in [68] revealed that despite of the sparse multipath environment, poor spatial correlation provides the significant capacity gain due to the planar wavefronts generated by near–field reflections at the ground receiver side.

In these studies, multiple antenna systems were used to combat fading in multipath propagation and to attain higher throughput. To achieve these objectives, the value of correlation coefficient due to fading at antenna elements provides insights about the achievable MIMO gain. In this case, large performance improvement can be achieved with low correlation coefficient. However, available literature is scarce for empirical evaluation of the correlation coefficient. Therefore, more measurement campaigns are required to study UAV–MIMO systems from the channel characterization viewpoint.

VI. Future Research Challenges

UAV propagation channels have significant importance in optimizing the coverage, reliability and capacity performance of UAV communication. Despite of all these advancements, many research issues remain open. In this section, we will discuss some research challenges and potential opportunities for characterizing UAV channels for future measurement campaigns and the development of realistic UAV channel model.

A. UAV Measurement Campaigns

Measurement campaigns are beneficial for the formulation of effective UAV channel models, evaluating the performance of UAV communication systems and network planning. However, propagation aspects of UAV communication change regionally due to UAV environment. In the literature, most of the UAV campaigns are launched in urban, suburban and open fields with mostly clear LOS conditions, whereas, measurement efforts are still missing for the dense–urban scenario, metropolitans with skyscrapers and over water bodies. Therefore, more extensive measurement campaigns are required. Moreover, the use of channel sounding equipment is important with regard to on–board space limitations, payload weight, bandwidth requirements and multipath resolution. To this end, channel characterization with USRP hardware, such as N–210 [46], B–210 [48], X–310 [102],[103] and B–200 mini can provide flexible platform due to lighter weight, low power consumption, wideband frequencies and capable to test different wireless communication protocols, such as multi–carrier and MIMO system in UAV communication framework. Other possible choices for channel measurement hardware used by different researchers are P410 UWB radio [47], autonomous mobile network scanner by Rohde & Schwarz [64] and 3G/4G enabled smart–phones [65],[74]. In addition, the effects of antenna placement on UAVs and the gain from UAV–MIMO system for both the AA and AG propagation are not well studied. Furthermore, the choice of aerial altitude platforms and different types of UAVs are another important aspects for both the UAV applications and channel characterization. In this case, multi–rotor and fixed–wing UAVs may be preferred for static and mobile UAV applications, respectively. However, for both types, the impact of UAV space and take–off weight (UAV weight with payload) can put constraints on the flight endurance time. Therefore, heavy–duty UAVs are more desirable to carry enough wireless equipment, for instance, DJI S–1000 and Agras MG–1 can accommodate a payload of around 7 kg and 10 kg, respectively. Also, UAVs should generate enough thrust to combat the atmospheric turbulence which may be detrimental in some UAV applications demanding stability for critical and continuous connectivity.

B. UAV Propagation Channel Models

Communication in UAV networks takes place over AA and AG channels. In this case, the AA channel is intended for the inter–UAV communication for coordination and collaboration in UAV swarms, while the AG channel is used for relaying data between UAVs and ground station. Most of the UAV propagation models are proposed with the approximation of time–invariant channels when non–stationarity is ignored in the estimation of the small–scale statistics, this may lead to erroneous conclusions. Therefore, it would be interesting to analyze the UAV propagation channel with the estimation of the stationary interval using temporal PDP correlation coefficient [71], correlation matrix distance [71], spectral divergence [104] and evolutionary spectrum [105] methods. Furthermore, the channel non–stationarity can be modeled by the flexibility of the geometric–based stochastic approach by considering time–variant parameters. The research on multidimensional UAV channel modeling is still in its preliminary stages as most of the empirical models reported large–scale statistical properties of the UAV channel with regard to flight dynamics, altitude and communication distance. Furthermore, airframe shadowing by small size rotary UAVs has not received commensurate level of attention and more empirical studies are required to study this phenomenon for both the AG channel in the single–hop network and the AA propagation in the multi–hop network. In addition, ray–tracing can be used to probe the airframe shadowing, as CAD tools are capable of incorporating UAV shape, metallic properties and different maneuvering positions.

VII. CONCLUSION

This paper has provided a comprehensive survey of the UAV channel characterization with measurement campaigns and statistical channel models. We have categorized the UAV channel measurement campaigns in low altitude platform based on the narrowband or wideband channel sounder, low–cost and low–power channel sounding solution, and widely deployed ground infrastructure. We have also reviewed empirical models for AG and AA propagation channels. Then we have classified the UAV channel modeling approaches as deterministic, stochastic and geometric–stochastic models. Further, we have examined some challenging issues in the practicability of UAV communications related to airframe shadowing, channel non–stationarity, and diversity techniques. Finally we have presented some future research challenges which will be helpful to provide further insight of the UAV channel characterization for launching future measurement campaigns and proposing pragmatic framework for the effective UAV channel models.

ACKNOWLEDGMENT

We would like to thank Dr Richard Staunton for reading our manuscript and correcting typographical errors.

REFERENCES

[1] Radio Technical Commission for Aeronautics (RTCA), SC-228, "Minimum Operational Performance Standards for Unmanned Aircraft Systems", May 2013, available online at http://www.rtca.org/content/sc-228.

[2] Radio Technical Commission for Aeronautics (RTCA), "Drone Advisory Committee (DAC)", 2016, available online at http://www.rtca.org/content/drone-advisory-committee.

[3] National Aeronautics and Space Administration, Oct. 2014, available online at http://www.aeronautics.nasa.gov/isrp/uas/index. html.

[4] A. Panagopoulos, P.D.M. Arapoglou, and P. Cottis, "Satellite Communications at KU, KA, and V bands: Propagation Impairments and Mitigation Techniques," *IEEE Commun. Surv. Tuts.*, vol. 6, no. 3, pp. 2-14, 2004.

[5] P. Chini, G. Giambene, and S. Kota, "A Survey on Mobile Satellite Systems," *Int. J. Satell. Commun. Networking*, vol. 28, no. 1, pp. 29-57, 2009.

[6] K. Daniel, M. Putzke, B. Dusza, and C. Wietfeld, "Three Dimensional Channel Characterization for Low Altitude Aerial Vehicles," in *Proc. 7th Int. Symp. Wireless Commun. Syst (ISWCS'10)*, York, UK, Sept. 2010, pp. 756-760.

[7] Q. Feng, J. McGeehan, E. K. Tameh, and A. R. Nix, "Path Loss Models for Air-to-Ground Radio Channels in Urban Environments," in *Proc. IEEE Veh. Technol Conf. (VTC-Spring'06)*, Melbourne, Australia, May 2006, pp. 2901-2905.

[8] Q. Feng, E. K. Tameh, A. R. Nix, and J. McGeehan, "Modelling the Likelihood of Line-of-Sight for Air-to-Ground Radio Propagation in Urban Environments," in *Proc. IEEE Global Commun. Conf. (GLOBECOM'06)*, San Francisco, USA, Dec. 2006, pp. 1-5.

[9] A. Al-Hourani, S. Kandeepan, and A. Jamalipour, "Modeling Air-to-Ground Path Loss for Low Altitude Platforms in Urban Environments," in *Proc. IEEE Global Commun. Conf. (GLOBECOM'14)*, Austin, USA, Dec. 2014, pp. 2898-2904.

[10] A. Al-Hourani, S. Kandeepan, and S. Lardner, "Optimal LAP Altitude for Maximum Coverage," *IEEE Wireless Commun. Lett.*, vol. 3, no. 6, pp. 569-572, 2014.

[11] A. Al-Hourani, S. Chandrasekharan, G. Kaandorp, W. Glenn, A. Jamalipour, and S. Kandeepan, "Coverage and Rate Analysis of Aerial Base Stations," *IEEE Trans. Aerosp. Electron. Syst.*, vol. 52, no. 6, pp. 3077-3081, 2016.

[12] M. Mozaffari, W. Saad, M. Bennis, and M. Debbah, "Efficient Deployment of Multiple Unmanned Aerial Vehicles for Optimal Wireless Coverage," *IEEE Commun. Lett.*, vol. 20, no. 8, pp. 1647-1650, 2016.

[13] D.W. Matolak and R. Sun, "Air-Ground Channel Characterization for Unmanned Aircraft Systems-Part I: Methods Measurements and Models for Over-Water Settings," *IEEE Trans. Veh. Technol.*, vol. 66, no. 1, pp. 26-44, 2017.

[14] R. Sun and D.W. Matolak, "Air-Ground Channel Characterization for Unmanned Aircraft Systems-Part II: Hilly and Mountainous Settings," *IEEE Trans. Veh. Technol.*, vol. 66, no. 3, pp. 1913-1925, 2017.

[15] D.W. Matolak and R. Sun, "Air-Ground Channel Characterization for Unmanned Aircraft Systems-Part III: The Suburban and Near-Urban Environments," *IEEE Trans. Veh. Technol.*, vol. 66, no. 8, pp. 6607-6618, 2017.

[16] W. Newhall and J. Reed, "A Geometric Air-to-Ground Radio Channel Model," in *Proc. IEEE Mil. Commun. Conf. (MILCOM'02)*, Anaheim, USA, Oct. 2002, pp. 632-636.

[17] M. Wentz and M. Stojanovic, "A MIMO Radio Channel Model for Low-Altitude Air-to-Ground Communication Systems," in *Proc. IEEE Veh. Technol Conf. (VTC-Fall'15)*, Boston, USA, Sept. 2015, pp. 1-6.

[18] M. Ibrahim and H. Arslan, "Air-Ground Doppler-Delay Spread Spectrum for dense scattering environments," in *Proc. IEEE Mil. Commun. Conf. (MILCOM'15)*, Tampa, USA, Oct. 2015, pp. 1661-1666.

[19] S. Gulfam, S. Nawaz, M. Patwary, and M. Maguid, "On the Spatial Characterization of 3-D Air-to-Ground Radio Communication Channels," in *Proc. IEEE Int. Conf. Commun. (ICC'15)*, London, UK, June 2015, pp. 2924-2930.

[20] L. Zeng, X. Cheng, C.X. Wang, and X. Yin, "A 3D Geometry-based Stochastic Channel Model for UAV-MIMO Channels," in *Proc. IEEE Wireless Commun. Netw. Conf. (WCNC'17)*, San Francisco, USA, March 2017, pp. 1-5.

[21] V.V. Chetlur and H.S. Dhillon, "Downlink Coverage Analysis for a Finite 3-D Wireless Network of Unmanned Aerial Vehicles," *IEEE Trans. Commun.*, vol. 65, no. 10, pp. 4543-4558, 2017.

[22] A. Mohammed, A. Mehmood, F. Pavlidou, and M. Mohorcic, "The Role of High-Altitude Platforms (HAPs) in the Global Wireless Connectivity," *Proc. IEEE*, vol. 99, no. 11, pp. 1939-1953, 2011.

[23] "Roadmap for the Integration of Civil Remotely-Piloted Aircraft Systems into the European Aviation System," EUROCONTROL, Brussels, Belgium, Tech. Rep., 2013, available online at https://publicintelligence.net/eu-rpa-roadmap/.

[24] US Department of Transportation Federal Aviation Authority, "Integration of Civil Unmanned Aircraft Systems (UAS) in the National Airspace System (NAS) Roadmap," 2013, available online at http://www.faa.gov/uas/media/uas_roadmap_2013.pdf.

[25] Civil Aviation Safety Authority (CASA), "Flying drones or model aircraft recreationally", available online at https://www.casa.gov.au/modelaircraft.

[26] M. Holzbock and C. Senninger, "An Aeronautical Multimedia Service Demonstration at High Frequencies," *IEEE Trans. Multimedia*, vol. 6, no. 4, pp. 20-29, 1999.

[27] Y. Lee, Y. Meng, and Y.H. Heng, "Experimental Characterizations of an Air to Land Channel Over Sea Surface in C Band," in *Proc. 29th USRI General Assembly*, 2008, pp. 2-5.

[28] Y.S. Meng and Y.H. Lee, "Study of Shadowing Effect by Aircraft Maneuvering," *Int. J. Electron. Commun.*, vol. 66, no. 1, pp. 7-11, 2012.

[29] J. Kunisch, I.de la Torre, A. Winkelmann, M. Eube, and T. Fuss, "Wideband Time–Variant Air–to–Ground Radio Channel Measurements at 5 GHz," in *Proc. 5th Eur. Conf. Antennas Propag. (EuCAP'11)*, Rome, Italy, April 2011, pp. 1386-1390.

[30] R.Sun and D.W. Matolak, "Air–Ground Channel Characterization for Unmanned Aircraft Systems Part–IV: Airframe Shadowing," *IEEE Trans. Veh. Technol.*, vol. 66, no. 9, pp. 7643-7652, 2017.

[31] J. Chen, B. Daneshrad, and W. Zhu, "MIMO Performance Evaluation for Airborne Wireless Communication Systems," in *Proc. IEEE Mil. Commun. Conf. (MILCOM'11)*, Baltimore, USA, Nov. 2011, pp. 1827-1832.

[32] M. Rice and M. Jensen, "Multipath Propagation for Helicopter-to-Ground MIMO Links," in *Proc. IEEE Mil. Commun. Conf. (MILCOM'11)*, Baltimore, USA, Nov. 2011, pp. 447-452.

[33] M. Rice and M. Saquib, "MIMO Equalization for Helicopter-to-Ground Communications," in *Proc. IEEE Mil. Commun. Conf. (MILCOM'11)*, Baltimore, USA, Nov. 2011, pp. 501-506.

[34] Y. Jiang, A. Tiwari, M. Rachid, and B. Daneshrad, "MIMO for Airborne Communications [Industry Perspectives]," *IEEE Wireless Commun.*, vol. 21, no. 5, pp. 4-6, 2014.

[35] W. Vergara, J. Levatich, and T. Carroll, "VHF Air–Ground Propagation Far Beyond the Horizon and Tropospheric Stability," *IRE Antennas Propag.*, vol. 10, no. 5, pp. 608–621, 1962.

[36] K. Chamberlin, "The Effect of Tree Cover on Air–Ground, VHF Propagation Path Loss," *IEEE Trans. Commun.*, vol. 34, no. 9, pp. 958-962, 1986.

[37] J.R. Child, "Air–to–ground propagation at 900 MHz," in *Proc. IEEE Veh. Technol Conf.(VTC–Fall'85)*, Colorado, USA, May 1985, pp. 73-80.

[38] M. Rice and R. Dye, "Narrowband Channel Model for Aeronautical Telemetry," *IEEE Trans. Aerosp. Electron. Syst.*, vol. 36, no. 4, pp. 1371-1376, 2000.

[39] W.G. Newhall, R. Mostafa, C. Dietrich, C.R. Anderson, G. Joshi, and J.H. Reed, "Wideband Air-to-Ground Radio Channel Measurements Using an Antenna Array at 2 GHz for Low-Altitude Operations," in *Proc. IEEE Mil. Commun. Conf. (MILCOM'03)*, Boston, USA, Oct. 2003, pp. 1422-1427.

[40] M. Rice, A. Davis, and C. Bettweiser, "Wideband Channel Model for Aeronautical Telemetry," *IEEE Trans. Aerosp. Electron. Syst.*, vol. 40, no. 1, pp. 57-69, 2004.

[41] M. Simunek, F.P. Fontan, and P. Pechac, "The UAV Low Elevation Propagation Channel in Urban Areas: Statistical Analysis and Time-Series Generator," *IEEE Trans. Antennas Propag.*, vol. 61, no. 7, pp. 3850-3858, 2013.

[42] M. Simunek, P. Pechac, and F.P. Fontan, "Excess Loss Model for Low Elevation Links in Urban Areas for UAVs," *Radio engineering*, vol. 20, no. 3, pp. 561-568, 2011.

[43] M. Simunek, F.P. Fontan, P. Pechac, and F.J.D. Otero, "Space Diversity Gain in Urban Area Low Elevation Links for Surveillance Applications," *IEEE Trans. Antennas Propag.*, vol. 61, no. 12, pp. 6255-6260, 2013.

[44] M. Simunek, P. Pechac, and F.P. Fontan, "Feasibility of UAV Link Space Diversity in Wooded Areas," *Intl. J. Antennas Propag.*, vol. 2013, pp. 1-6, 2013.

[45] X. Cai, A.G-. Plaza, D. Alonso, L. Zhang, C.B. Rodriguez, A.P. Yuste, and X. Yin, "Low Altitude UAV Propagation Channel Modelling," in *Proc. 11th Eur. Conf. Antennas Propag (EuCAP'17)*, Paris, France, March 2017, pp. 1443-1447.

[46] X. Ye, X. Cai, X. Yin, J. R. Pineiro, L. Tian, and J. Dou, "Air-to-Ground Big-Data-Assisted Channel Modeling Based on Passive Sounding in LTE Networks," in *Proc. IEEE Global Commun. Conf. (GLOBECOM'17)*, Singapore, Dec. 2017, pp. 1-6.

[47] W. Khawaja, I. Guvenc, and D. Matolak, "UWB Channel Sounding and Modeling for UAV Air-to-Ground Propagation Channels," in *Proc. IEEE Global Commun. Conf. (GLOBECOM'16)*, Washington, USA, Dec. 2016, pp. 1-7.

[48] R.M. Gutierrez, H. Yu, Y. Rong, and D.W. Bliss, "Time and Frequency Dispersion Characteristics of the UAS Wireless Channel in Residential and Mountainous Desert Terrains," in *Proc. IEEE Annual Consumer Commun. Netw. Conf. (CCNC'17)*, Las Vegas, USA, Jan. 2017, pp. 516-521.

[49] E.W. Frew and T.X. Brown, "Airborne Communication Networks for Small Unmanned Aircraft Systems," *Proceedings of the IEEE*, vol. 96, no. 12, pp. 2008-2027, 2008.

[50] N. Goddemeier, S. Rohde, and C. Wietfeld, "Experimental Validation of RSS Driven UAV Mobility Behaviors in IEEE 802.11s Networks," in *Proc. IEEE Global Commun. Conf. (GLOBECOM'12)*, Anaheim, USA, Dec. 2012, pp. 1550-1555.

[51] E. Yanmaz, S. Hayat, J. Scherer, and C. Bettstetter, "Experimental Performance Analysis of Two-Hop Aerial 802.11 Networks,"in *Proc. IEEE Wireless Commun. Netw. Conf. (WCNC'14)*, Istanbul, Turkey, April 2014, pp. 3118-3123.

[52] T. Brown, B. Argrow, C. Dixon, S. Doshi, R. Thekkekunnel, and D. Henkel, "Ad-hoc UAV Ground Network (Augnet)," in *Proc. AIAA Unmanned Unlimited Tech. Conf.*, 2004, pp. 29-39.

[53] S. Hayat, E. Yanmaz, and C. Bettstetter, "Experimental Analysis of Multipoint-to-Point UAV Communications with IEEE 802.11n and 802.11ac," in *Proc. 26th IEEE Annual Intl. Symp. Personal Indoor Mobile Radio Commun. (PIMRC'15)*, Hong Kong, 2015. pp. 1991-1996.

[54] J. Allred, A. B. Hasan, S. Panichsakul, W. Pisano, P. Gray, and J. Huang, "SensorFlock: An Airborne Wireless Sensor Network of Micro-Air Vehicle," in *Proc. ACM SenSys*, 2007, pp. 117–129.

[55] A. Shaw and K. Mohseni, "A Fluid Dynamic Based Coordination of a Wireless Sensor Network of Unmanned Aerial Vehicles: 3-D Simulation and Wireless Communication Characterization," *IEEE Sensors Journal*, vol. 11, no. 3, pp. 722-736, 2011.

[56] N. Ahmed, S. Kanhere, and S. Jha, "On the Importance of Link Characterization for Aerial Wireless Sensor Network," *IEEE Commun. Mag.*, vol. 54, no. 5, pp. 52-57, 2016.

[57] N. Goddemeier and C. Wietfeld, "Investigation of Air–to–Air Channel Characteristics and a UAV Specific Extension to the Rice Model," in *Proc. IEEE Global Commun. Conf. (GLOBECOM'15)*, San Diego, USA, Dec. 2015, pp. 1-5.

[58] E. Yanmaz, R. Kuschnig, and C. Bettstetter, "Channel Measurements over 802.11a–based UAV–to–Ground Links," in *Proc. IEEE Global Commun. Conf. (GLOBECOM'11)*, Houston, USA, Dec. 2011, pp. 1280-1284.

[59] E. Yanmaz, R. Kuschnig, and C. Bettstetter, "Achieving Air–Ground Communications in 802.11 Networks with Three-Dimensional Aerial Mobility," in *Proc. IEEE INFOCOM*, Turin, Italy, April 2013, pp. 120-124.

[60] C.M. Cheng, P.H. Hsiao, H. Kung, and D. Vlah, "Performance Measurement of 802.11a Wireless Links from UAV to Ground Nodes with Various Antenna Orientations," in *Proc. Intl. Conf. Computer Comm. and Networks (ICCCN'06)*, Arlington, USA, Oct. 2006, pp. 303-308.

[61] D. Hague, H. Kung, and B. Suter, "Field Experimentation of Cots-Based UAV Networking," in *Proc. IEEE Mil. Commun. Conf. (MILCOM'06)*, Washington, USA, Oct. 2006, pp. 1-7.

[62] N. Goddemeier, K. Daniel, and C. Wietfeld, "Coverage Evaluation of Wireless Networks for Unmanned Aerial Systems," in *Proc. IEEE Global Commun. Conf. (GLOBECOM'10)*, Miami, USA, Dec. 2010, pp. 1760-1765.

[63] T. Tavares, P. Sebastiao, N. Souto, F. Cercas, M. Ribeiro, A. Correia, and F.J. Velez, "Generalized LUI Propagation Model for UAVs Communications using Terrestrial Cellular Networks," in *Proc. IEEE Veh. Technol Conf. (VTC–Fall'15)*, Boston, USA, Sept. 2015, pp. 1-6.

[64] R. Amorim, H. Nguyen, P. Mogensen, I.Z. Kovacs, J. Wigard, and T.B. Sorensen, "Radio Channel Modeling for UAV Communication Over Cellular Networks," *IEEE Wireless Commun. Lett.*, vol. 6, no. 4, pp. 514-517, 2017.

[65] A.Al-Hourani and K. Gomez, "Modeling Cellular–to–UAV Path-Loss for Suburban Environments," *IEEE Wireless Commun. Lett.*, vol. 7, no. 1, pp. 82-85, 2018.

[66] E. Teng, J.D. Falcao, and B. Iannucci, "Holes–in–the–Sky: A Field Study on Cellular-Connected UAS," in *Proc. (ICUAS'17)*, Miami, USA, June 2017, pp. 1165-1174.

[67] H.T. Kung, C.K. Lin, T.H. Lin, S.J. Tarsa, and D. Vlah, "Measuring Diversity on a Low–Altitude UAV in a Ground–to–Air Wireless

802.11 Mesh Network," in *Proc. IEEE Global Commun. Conf. (GLOBECOM'10)*, Miami, USA, Dec. 2010, pp. 1799-1804.

[68] T.J. Willink, C. Squires, G. Colman, and M. Muccio, "Measurement and Characterization of Low-Altitude Air-to-Ground MIMO Channels," *IEEE Trans. Veh. Technol.*, vol. 65, no. 4, pp. 2637-2648, 2016.

[69] L. Gupta, R. Jain, and G. Vaszkun, "Survey of Important Issues in UAV Communication Networks," *IEEE Commun. Sur. Tut.*, vol. 18, no. 2, pp. 1123-1152, 2016.

[70] S. Hayat, E. Yanmaz, and R. Muzaffar, "Survey on Unmanned Aerial Vehicle Networks for Civil Applications: A Communications Viewpoint," *IEEE Commun. Sur. Tut.* vol. 18, no. 4, pp. 2624-2661, 2016.

[71] D.W. Matolak, "Air-Ground Channels and Models: Comprehensive Review and Considerations for Unmanned Aircraft Systems," in *Proc. IEEE Aero. Conf.*, MT, USA, March 2012, pp. 1-17.

[72] Qualcomm Technologies Inc., "LTE Unmanned Aircraft Systems Trial Report," 2017, available online at https://www.qualcomm.com/documents/lte-unmanned-aircraft-systems-trial-report.

[73] Ericsson, "Ericsson and China Mobile conduct world's first 5G drone prototype field trial", 2016, available online at https://www.ericsson.com/en/news/2016/8/ericsson-and-china-mobile-conduct-worlds-first-5g-drone-prototype-field-trial-.

[74] L. Afonso, N. Souto, P. Sebastiao, M. Ribeiro, T. Tavares, and R. Marinheiro, "Cellular for the Skies: Exploiting Mobile Network Infrastructure for Low Altitude Air–to–Ground Communications," *IEEE Aerosp. Electron. Syst.*, vol. 31, no. 8, pp. 4-11, 2016.

[75] I. Bor-Yaliniz and H. Yanikomeroglu, "The New Frontier in RAN Heterogeneity: Multi-Tier Drone-Cells," *IEEE Commun. Mag.*, vol. 54, no. 11, pp. 48-55, 2016.

[76] L. Bekmezci, O. K. Sahingoz, and S. Temel, "Flying Ad-hoc Networks (FANETs): A Survey," *Ad Hoc Netw.*, vol. 11, no. 3, pp. 1254-1270, 2013.

[77] A. Kaadan, H.H. Refai, and P.G. LoPresti, "Multielement FSO Transceivers Alignment for Inter-UAV Communications," *J. of lightw. Technol.*, vol. 32, no. 24, pp. 4183-4193, 2014.

[78] Z. Xiao, P. Xia, and X.-gen Xia, "Enabling UAV Cellular with Millimeter-Wave Communication: Potentials and Approaches," *IEEE Commun. Mag.*, vol. 54, no. 5, pp. 66-73, 2016.

[79] I. Y. Abualhaol and M. M. Matalgah, "Performance Analysis of Multi-Carrier Relay-Based UAV Network over Fading Channels," in *Proc. IEEE Global Commun. Conf. (GLOBECOM'10)*, Miami, USA, Dec. 2010, pp. 1811-1815.

[80] F. Jiang and A. L. Swindlehurst, "Optimization of UAV Heading for the Ground-to-Air Uplink," in *IEEE J. Sel. Areas Commun.*, vol. 30, no. 5, pp. 993-1005, 2012.

[81] Y. Zhou, J. Li, L. Lamont, and C. Rabbath, "Modeling of Packet Dropout for UAV Wireless Communications," in *Proc. IEEE Intl. Conf. Ntw. Commun. (ICNC'12)*, Maui, USA, Feb. 2012, pp. 677-682.

[82] I. Sen and D. Matolak, "Vehicle-Vehicle Channel Models for the 5-GHz Band," in *IEEE Trans. Intell. Trans. Sys.*, vol. 9, no. 2, 2008, pp. 235-245.

[83] I. Bor-Yaliniz, S.S. Szyszkowicz, and H. Yanikomeroglu, "Environment-Aware Drone-Base-Station Placements in Modern Metropolitans," *IEEE Wireless Commun. Lett.*, vol. 7, no. 3, pp. 372-375, 2018.

[84] A.M. Hayajneh, S.A.R. Zaidi, D.C. McLernon, and M. Ghogho, "Optimal Dimensioning and Performance Analysis of Drone-Based Wireless Communications," in *Proc. IEEE Global Commun. Conf. (GLOBECOM'16)*, Washington, USA, Dec. 2016, pp. 1-6.

[85] M. Alzenad, A. El-Keyi, F. Lagum, and H. Yanikomeroglu, "3-D Placement of an Unmanned Aerial Vehicle Base Station (UAV-BS) for Energy-Efficient Maximal Coverage," *IEEE Wireless Commun. Lett.*, vol. 6, no. 4, pp. 434-437, 2016.

[86] M. Mozaffari, W. Saad, M. Bennis, and M. Debbah, "Optimal Transport Theory for Power-Efficient Deployment of Unmanned Aerial Vehicles," in *Proc. IEEE Int. Conf. Commun. (ICC'16)*, Kuala Lumpur, Malaysia, May 2016, pp. 1-6.

[87] J. Lu, S. Wan, X. Chen, and P. Fan, "Energy-Efficient 3D UAV-BS Placement versus Mobile User's Density and Circuit Power," in *Proc. IEEE Global Commun. Conf. (GLOBECOM'17)*, Singapore, Dec. 2017, pp. 1-6.

[88] M. Mozaffari, W. Saad, M. Bennis, and M. Debbah, "Drone Small Cells in the Clouds: Design, Deployment and Performance Analysis," in *Proc. IEEE Global Commun. Conf. (GLOBECOM'15)*, San Diego, USA, Dec. 2015, pp. 1-6.

[89] M. Mozaffari, W. Saad, M. Bennis, and M. Debbah, "Optimal Transport Theory for Cell Association in UAV-Enabled Cellular Networks," *IEEE Commun. Lett.*, vol. 21, no. 9, pp. 2053-2056, 2017.

[90] M. Mozaffari, W. Saad, M. Bennis, and M. Debbah, "Wireless Communication Using Unmanned Aerial Vehicles (UAVs): Optimal Transport Theory for Hover Time Optimization," *IEEE Trans. Wireless Commun.*, vol. 16, no. 12, pp. 8052-8066, 2017.

[91] Y. Chen, W. Feng, and G. Zheng, "Optimum Placement of UAV as Relays, "*IEEE Commun. Lett.*, vol. 22, no. 2, pp. 248-251, 2018.

[92] R. Irem Bor-Yaliniz, A. El-Keyi, and H. Yanikomeroglu, "Efficient 3-D Placement of an Aerial Base Station in Next Generation Cellular Networks," in *Proc. IEEE Int. Conf. Commun. (ICC'16)*, Kuala Lumpur, Malaysia, May 2016, pp. 1-5.

[93] M. Chen, M. Mozaffari, W. Saad, C. Yin, M. Debbah, and C.S. Hong, "Caching in the Sky: Proactive Deployment of Cache-Enabled Unmanned Aerial Vehicles for Optimized Quality-of-Experience," *IEEE J. Sel. Areas Commun.*, vol. 35, no. 5, pp. 1046-1061, 2017.

[94] Y. Zeng, R. Zhang, and T. J. Lim, "Wireless Communications with Unmanned Aerial Vehicles: Opportunities and Challenges," *IEEE Wireless Commun. Mag.*, vol. 54, no. 5, pp. 36–42, 2016.

[95] S. Elnoubi, "A Simplified Stochastic Model for the Aeronautical Mobile Radio Channel," in *Proc. IEEE Vehicular Tech. Conf. (VTC'92)*, Denver, USA, May 1992, vol. 2, pp. 960-963.

[96] M. A. Zaman, S. A. Mamun, M. Gaffar, M. M. Alam, and M. I. Momtaz, "Modeling VHF Air–to–Ground Multipath Propagation Channel and Analyzing Channel Characteristics and BER Performance," in *Proc. IEEE Region 8 SIBIRCON*, Listvyanka, Russia, July 2010, pp. 335-338.

[97] Y. Ding, Y. Xiao, J. Xie, and T. Zhang, "A Time-Varying Transition Channel Model for Air-Ground Communication," in *Proc. IEEE Digital Avionics Sys. Conf. (DASC'17)*, St. Petersburg, USA, Sept. 2017, pp. 1-8.

[98] S. Blandino, F. Kaltenberger, and M. Feilen, "Wireless Channel Simulator Testbed for Airborne Receivers," in *Proc. IEEE Global Commun. Conf. (GLOBECOM'15)*, San Diego, USA, Dec. 2015, pp. 1-6.

[99] X. Gao, Z. Chen, and Y. Hu, "Analysis of Unmanned Aerial Vehicle MIMO Channel Capacity Based on Aircraft Attitude," *WSEAS Trans. Inform. Sci. Appl.*, vol. 10, pp. 58-67, 2013.

[100] M. Mozaffari, W. Saad, M. Bennis, and M. Debbah, "Unmanned Aerial Vehicle with Underlaid Device-to-Device Communications: Performance and Tradeoffs, "*IEEE Trans. Wireless Commun.*, vol. 15, no. 6, pp. 3949-3963, 2016.

[101] F. Lagum, I. Bor-Yaliniz, and H. Yanikomeroglu, "Strategic Densification with UAV-BSs in Cellular Networks," *IEEE Wireless. Commun. Lett.*, vol. 7, no. 3, pp. 384-387, 2018.

[102] B.V.D. Bergh, A. Chiumento, and S. Pollin, "LTE in the sky: trading off propagation benefits with interference costs for aerial nodes," *IEEE Commun. Mag.*, vol. 54, no. 5, pp. 44-50, 2016.

[103] W. Khawaja, O. Ozdemir, and I. Guvenc, "UAV Air-to-Ground Channel Characterization for mmWave Systems," in *Proc. IEEE Vehicular Tech. Conf. (VTC-Fall'17)*, Toronto, Canada, Sept. 2017, pp. 1-5.

[104] T.T. Georgiou, "Distances and Riemannian metrics for spectral density functions," *IEEE Trans. Signal Process.*, vol. 55, no. 8, pp. 3995-4003, 2007.

[105] T.J. Willink, "Wide sense stationarity of mobile MIMO radio channels," *IEEE Trans. Veh. Technol.*, vol. 57, no. 2, pp. 704-714, 2008.

Aziz Altaf Khuwaja received his B.E. degree in Telecommunication engineering from Mehran University of Engineering & Technology, Jamshoro, Pakistan, in 2010 and M.Sc. from the University of Nottingham, U.K. in 2015. He is currently pursuing Ph.D. in Engineering at the School of Engineering, the University of Warwick, U.K. He is also working as an Assistant Professor at the Department of Electrical Engineering, Sukkur IBA University, Sukkur, Pakistan. His research interests include wireless communications and radio resource management in UAV communications.

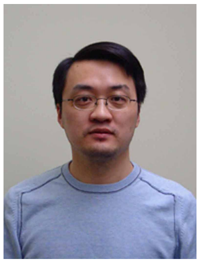

Yunfei Chen (S'02-M'06-SM'10) received his B.E. and M.E. degrees in electronics engineering from Shanghai Jiaotong University, Shanghai, P.R.China, in 1998 and 2001, respectively. He received his Ph.D. degree from the University of Alberta in 2006. He is currently working as an Associate Professor at the University of Warwick, U.K. His research interests include wireless communications, cognitive radios, wireless relaying and energy harvesting.

Nan Zhao (S'08-M'11-SM'16) is currently an Associate Professor in the School of Information and Communication Engineering at Dalian University of Technology, China. He received the B.S. degree in electronics and information engineering in 2005, the M.E. degree in signal and information processing in 2007, and the Ph.D. degree in information and communication engineering in 2011, from Harbin Institute of Technology, Harbin, China. His recent research interests include interference alignment, wireless power transfer, and physical layer security.

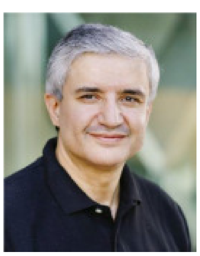

Mohamed-Slim Alouini (S'94-M'98-SM'03-F'09) was born in Tunis, Tunisia. He received the Ph.D. degree in Electrical Engineering from the California Institute of Technology (Caltech), Pasadena, CA, USA, in 1998. He served as a faculty member in the University of Minnesota, Minneapolis, MN, USA, then in the Texas A&M University at Qatar, Education City, Doha, Qatar before joining King Abdullah University of Science and Technology (KAUST), Thuwal, Makkah Province, Saudi Arabia as a Professor of Electrical Engineering in 2009. His current research interests include the modeling, design, and performance analysis of wireless communication system.